OPEN ACCESS Freely available online

PLoS one

The ESCRT System Is Required for Hepatitis C Virus Production

Yasuo Ariumi[1]*, Misao Kuroki[1], Masatoshi Maki[2], Masanori Ikeda[1], Hiromichi Dansako[1], Takaji Wakita[3], Nobuyuki Kato[1]

1 Department of Tumor Virology, Okayama University Graduate School of Medicine, Dentistry, and Pharmaceutical Sciences, Okayama, Japan, **2** Department of Applied Molecular Biosciences, Graduate School of Bioagricultural Sciences, Nagoya University, Nagoya, Japan, **3** Department of Virology II, National Institute of Infectious Diseases, Tokyo, Japan

Abstract

Background: Recently, lipid droplets have been found to be involved in an important cytoplasmic organelle for hepatitis C virus (HCV) production. However, the mechanisms of HCV assembly, budding, and release remain poorly understood. Retroviruses and some other enveloped viruses require an endosomal sorting complex required for transport (ESCRT) components and their associated proteins for their budding process.

Methodology/Principal Findings: To determine whether or not the ESCRT system is needed for HCV production, we examined the infectivity of HCV or the Core levels in culture supernatants as well as HCV RNA levels in HuH-7-derived RSc cells, in which HCV-JFH1 can infect and efficiently replicate, expressing short hairpin RNA or siRNA targeted to tumor susceptibility gene 101 (TSG101), apoptosis-linked gene 2 interacting protein X (Alix), Vps4B, charged multivesicular body protein 4b (CHMP4b), or Brox, all of which are components of the ESCRT system. We found that the infectivity of HCV in the supernatants was significantly suppressed in these knockdown cells. Consequently, the release of the HCV Core into the culture supernatants was significantly suppressed in these knockdown cells after HCV-JFH1 infection, while the intracellular infectivity and the RNA replication of HCV-JFH1 were not significantly affected. Furthermore, the HCV Core mostly colocalized with CHMP4b, a component of ESCRT-III. In this context, HCV Core could bind to CHMP4b. Nevertheless, we failed to find the conserved viral late domain motif, which is required for interaction with the ESCRT component, in the HCV-JFH1 Core, suggesting that HCV Core has a novel motif required for HCV production.

Conclusions/Significance: These results suggest that the ESCRT system is required for infectious HCV production.

Citation: Ariumi Y, Kuroki M, Maki M, Ikeda M, Dansako H, et al. (2011) The ESCRT System Is Required for Hepatitis C Virus Production. PLoS ONE 6(1): e14517. doi:10.1371/journal.pone.0014517

Editor: Gian Maria Fimia, INMI, Italy

Received May 6, 2010; **Accepted** December 15, 2010; **Published** January 11, 2011

Funding: This work was supported by a Grant-in-Aid for Scientific Research (C) from the Japan Society for the Promotion of Science (JSPS), by a Grant-in-Aid for Research on Hepatitis from the Ministry of Health, Labor, and Welfare of Japan, by the Viral Hepatitis Research Foundation of Japan, by the Kawasaki Foundation for Medical Science, Medical Welfare, by the Okayama Medical Foundation, and by Ryobi Teien Memory Foundation. MK was supported by a Research Fellowship from the JSPS for Young Scientists. The funders had no role in study design, data collection and analysis, decision to publish, or preparation of the manuscript.

Competing Interests: The authors have declared that no competing interests exist.

* E-mail: ariumi@md.okayama-u.ac.jp

Introduction

Hepatitis C virus (HCV) is a causative agent of chronic hepatitis, which progresses to liver cirrhosis and hepatocellular carcinoma. HCV is an enveloped virus with a positive single stranded 9.6 kb RNA genome, which encodes a large polyprotein precursor of approximately 3,000 amino acid residues. This polyprotein is cleaved by a combination of the host and viral proteases into at least 10 proteins in the following order: Core, envelope 1 (E1), E2, p7, nonstructural protein 2 (NS2), NS3, NS4A, NS4B, NS5A, and NS5B [1]. HCV Core, a highly basic RNA-binding protein, forms a viral capsid and is targeted to lipid droplets [2–6]. The Core is essential for infectious virion production [7]. NS5A, a membrane-associated RNA-binding phosphoprotein, is also involved in the assembly and maturation of infectious HCV particles [8,9]. Intriguingly, NS5A is a key regulator of virion production through the phosphorylation by casein kinase II [9]. Recently, lipid droplets have been found to be involved in an important cytoplasmic organelle for HCV production [4]. Indeed, NS5A is known to colocalize with the Core on lipid droplets [5], and the interaction between NS5A and the Core is critical for the production of infectious HCV particles [3]. However, the host factor involved in HCV assembly, budding, and release remains poorly understood.

Budding is an essential step in the life cycle of enveloped viruses. Endosomal sorting complex required for transport (ESCRT) components and associated factors, such as tumor susceptibility gene 101 (TSG101, a component of ESCRT-I), charged multivesicular body protein 4b (CHMP4b, a component of ESCRT-III), and apoptosis-linked gene 2 interacting protein X (ALIX, a TSG101- and CHMP4b-binding protein), have been found to be involved in membrane remodeling events that accompany endosomal protein sorting, cytokinesis, and the budding of several enveloped viruses, such as human immunodeficiency virus type 1 (HIV-1) [10–12]. The ESCRT complexes I, II, and III are sequentially, or perhaps concentrically recruited to the endosomal membrane to sequester

cargo proteins and drive vesicularization into the endosome. Finally, ESCRT-III recruits Vps4 (two isoforms, Vps4A and Vps4B), a member of the AAA-family of ATPase that disassembles and thereby terminates and recycles the ESCRT machinery.

Since HCV is also an enveloped RNA virus, we hypothesized that the ESCRT system might be required for HCV production. To test this hypothesis, we examined the release of HCV Core into culture supernatants from cells rendered defective for ESCRT components by RNA interference. The results provide evidence that the ESCRT system is required for HCV production.

Materials and Methods

Cell Culture

293FT cells (Invitrogen, Carlsbad, CA) were cultured in Dulbecco's modified Eagle's medium (DMEM; Invitrogen) supplemented with 10% fetal bovine serum (FBS). The HuH-7-derived cell line, RSc cured cells that cell culture-generated HCV-JFH1 (JFH1 strain of genotype 2a) [13] could infect and effectively replicate [14–16] and OR6c and OR6 cells harboring the genome-length HCV-O RNA with luciferase as a reporter were cultured in DMEM with 10% FBS as described previously [17,18].

Plasmid Construction

To construct pcDNA3-FLAG-Alix, a DNA fragment encoding Alix was amplified from total RNAs derived from RSc cells by RT-PCR using the follwing pairs of primers: Forward 5′-CGGGATCCAAGATGGCGACATTCATCTCGGT-3′ and reverse 5′-CCGGCGGCCGCTTACTGCTGTGGATAGTAAG-3′. The obtained DNA fragment was subcloned into *Bam*HI-*Not*I of pcDNA3-FLAG vector [19], and the nucleotide sequences were determined by Big Dye termination cycle sequencing using an ABI Prism 310 genetic analyzer (Applied Biosystems, Foster City, CA, USA). The plasmid of pJRN/3-5B was based on pJFH1 [13] and was constructed as previously described [20].

RNA synthesis, RNA transfection, and Selection of G418-resistant cells

Plasmid pJRN/3-5B were linearized by *Xba*I and used for the RNA synthesis with the T7 MEGAScript kit (Ambion, Austin, TX). *In vitro* transcribed RNA was transfected into OR6c cells by electroporation [17,18]. The transfected cells were selected in culture medium containing G418 (0.3 mg/ml) for 3 weeks. We referred to them as OR6c/JRN 3-5B cells.

Immunofluorescence and Confocal Microscopic Analysis

Cells were fixed in 3.6% formaldehyde in phosphate-buffered saline (PBS) and permeabilized in 0.1% Nonidet P-40 (NP-40) in PBS at room temperature as previously described [21]. Cells were incubated with anti-HCV Core antibody (CP-9 and CP-11 mixture; Institute of Immunology, Tokyo, Japan), anti-Myc-Tag antibody (PL14; Medical & Biological Laboratories, MBL, Nagoya, Japan), anti-Alix antibody (Covalab, Villeurbanne, France), and/or anti-FLAG polyclonal antibody (Sigma, St. Louis, MO) at a 1:300 dilution in PBS containing 3% bovine serum albumin (BSA) at 37°C for 30 min. Cells were then stained with fluorescein isothiocyanate (FITC)-conjugated anti-rabbit antibody (Jackson ImmunoResearch, West Grove, PA) or anti-Cy3-conjugated anti-mouse antibody (Jackson ImmunoResearch) at a 1:300 dilution in PBS containing BSA at 37°C for 30 min. Lipid droplets and nuclei were stained with BODIPY 493/503 (Molecular Probes, Invitrogen) and DAPI (4′,6′-diamidino-2-phenylindole), respectively. Following extensive washing in PBS, cells were mounted on slides using a mounting media of 90% glycerin/10% PBS with 0.01% *p*-phenylenediamine added to reduce fading. Samples were viewed under a confocal laser-scanning microscope (LSM510; Zeiss, Jena, Germany).

RNA Interference

The following siRNAs were used: human TSG101 (siGENOME SMARTpool M-003549-01-0005 and 5′-CCUCCAGUCUUCUCUCGUCUU-3′ sense, 5′-GACGAGAGAAGACUGGAGGUU-3′ antisense), human Alix/PDCD6IP (siGENOME SMARTpool M-004233-02-0005), human Vps4B (siGENOME SMARTpool M-013119-02-0005), human CHMP4b (siGENOME SMARTpool M-018075-00-0005), and siGENOME Non-Targeting siRNA Pool#1 (D-001206-13-05) (Dharmacon, Thermo Fisher Scientific, Waltham, MA) as a control. siRNAs (50 nM final concentration) were transiently transfected into either RSc cells [14–16] or OR6 cells [17,18] using Oligofectamine (Invitrogen) according to the manufacturer's instructions. Oligonucleotides with the following sense and antisense sequences were used for the cloning of short hairpin (sh) RNA-encoding sequences against TSG101, Alix, Vps4B, or CHMP4b in lentiviral vector: TSG101i, 5′-GATCCCC GGAGGAAATGGATCGTGCCTTCAAGAGAGGCACGATCCATTTCCTCCTTTTTGGAAA-3′ (sense), 5′-AGCTTTTCCAAAAAGGAGGAAATGGATCGTGCCTCTCTTGAAGGCACGATCCATTTCCTCCGGG-3′ (antisense); Alixi, 5′-GATCCCC GGAGGTGTTCCCTGTCTTGTTCAAGAGACAAGACAGGGAACACCTCCTTTTTGGAAA-3′ (sense), 5′-AGCTTTTCCAAAAAGGAGGTGTTCCCTGTCTTGTCTCTTGAACAAGACAGGGAACACCTCCGGG-3′ (antisense); Vps4Bi, 5′-GATCCCC GGAGAATCTGATGATCCTGTTCAAGAGACAGGATCATCAGATTCTCCTTTTTGGAAA-3′ (sense), 5′-AGCTTTTCCAAAAAGGAGAATCTGATGATCCTGTCTCTTGAACAGGATCATCAGATTCTCCGGG-3′ (antisense); CHMP4bi, 5′-GATCCCC GAGGAGGACGACGACATGATTCAAGAGATCATGTCGTCGTCCTCCTCTTTTTGGAAA-3′ (sense), 5′-AGCTTTTCCAAAAAGAGGAGGACGACGACATGATCTCTTGAATCATGTCGTCGTCCTCCTCGGG-3′ (antisense); Broxi, 5′-GATCCCCGGATGACAGTACTAAACCCTTCAAGAGAGGGTTTAGTACTGTCATCCTTTTTGGAAA-3′ (sense), 5′-AGCTTTTCCAAAAAGGATGACAGTACTAAACCCTCTCTTGAAGGGTTTAGTACTGTCATCCGGG-3′ (antisense). The oligonucleotides above were annealed and subcloned into the *Bgl*II-*Hin*dIII site, downstream from an RNA polymerase III promoter of pSUPER [22], to generate pSUPER-TSG101i, pSUPER-Alixi, pSUPER-Vps4Bi, and pSUPER-CHMP4bi, respectively. To construct pLV-TSG101i, pLV-Alixi, pLV-Vps4Bi, and pLV-CHMP4bi, the *Bam*HI-*Sal*I fragments of the corresponding pSUPER plasmids were subcloned into the *Bam*HI-*Sal*I site of pRDI292 [23], an HIV-1-derived self-inactivating lentiviral vector containing a puromycin resistant marker allowing for the selection of transduced cells, respectively.

Lentiviral Vector Production

The vesicular stomatitis virus (VSV)-G-pseudotyped HIV-1-based vector system has been described previously [24–26]. The lentiviral vector particles were produced by transient transfection of the second-generation packaging construct pCMV-ΔR8.91 [24–26] and the VSV-G-envelope-expressing plasmid pMDG2 as well as pRDI292 into 293FT cells with FuGene6 (Roche Diagnostics, Basel, Switzerland).

HCV Infection Experiments

The supernatants was collected from cell culture-generated HCV-JFH1 [13]-infected RSc cells [14–16] at 5 days post-

infection and stored at −80°C after filtering through a 0.45 μm filter (Kurabo, Osaka, Japan) until use. For infection experiments with HCV-JFH1 virus, RSc cells (1×10^5 cells/well) were plated onto 6-well plates and cultured for 24 hours (hrs). Then, we infected the cells with 50 μl (equivalent to a multiplicity of infection [MOI] of 0.1) of inoculum. The culture supernatants were collected and the levels of HCV Core were determined by enzyme-linked immunosorbent assay (ELISA) (Mitsubishi Kagaku Bio-Clinical Laboratories, Tokyo, Japan). Total RNA was isolated from the infected cellular lysates using RNeasy mini kit (Qiagen, Hilden, Germany) for quantitative RT-PCR analysis of intracellular HCV RNA. The infectivity of HCV in the culture supernatants was determined by a focus-forming assay at 48 hrs post-infection. The HCV infected cells were detected using anti-HCV Core antibody (CP-9 and CP-11). Intracellular HCV infectivity was determined by a focus-forming assay at 48 hrs post-inoculation of lysates by repeated freeze and thaw cycles (three times).

Quantitative RT-PCR Analysis

The quantitative RT-PCR analysis for HCV RNA was performed by real-time LightCycler PCR (Roche) as described previously [17,18]. We used the following forward and reverse primer sets for the real-time LightCycler PCR: TSG101, 5′-ATGGCGGTGTCGGAGAGCCA-3′ (forward), 5′-AACAGGTTTGAGATCTTTGT-3′ (reverse); Alix, 5′-ATGGCGACATTCATCTCGGT-3′ (forward), 5′-TACTGGGCCTGCTCTTCCCC-3′ (reverse); Vps4B, 5′-ATGTCATCCACTTCGCCCAA-3′ (forward), 5′-ATACTGCACAGCATGCTGAT-3′ (reverse); CHMP4b, 5′-ATGTCGGTGTTCGGGAAGCT-3′ (forward), 5′-ATCTCTTCCGTGTCCCGCAG-3′ (reverse); Brox, 5′-ATGACCCATTGGTTTCATAG-3′ (forward), 5′-CCTGGATGACCTCAAGTCAT-3′ (reverse); β-actin, 5′-TGACGGGGTCACCCACACTG-3′ (forward), 5′-AAGCTGTAGCCGCGCTCGGT-3′ (reverse); and HCV-JFH1, 5′-AGAGCCATAGTGGTCTGCGG-3′ (forward), 5′-CTTTCGCAACCCAACGCTAC-3′ (reverse).

MTT Assay

Cells (5×10^3 cells/well) were plated onto 96-well plates and cultured for 24, 48 or 72 hrs, then, subjected to the colorimetric 3-(4,5-dimethylthiazol-2-yl)-2,5-diphenyltetrazolium bromid (MTT) assay according to the manufacturer's instructions (Cell proliferation kit I, Roche). The absorbance was read using a microplate reader (Multiskan FC, Thermo Fisher Scientific) at 550 nm with a reference wavelength of 690 nm.

Renilla Luciferase (RL) Assay

OR6 cells (1.5×10^4 cells/well) [17,18] were plated onto 24-well plates and cultured for 24 hrs. The cells were transfected with siRNAs (50 nM) using Oligofectamine and incubated for 72 hrs, then, subjected to the RL assay according to the manufacturer's instructions (Promega, Madison, WI). A lumat LB9507 luminometer (Berthold, Bad Wildbad, Germany) was used to detect RL activity.

Western Blot Analysis

Cells (2×10^5 cells/well) were plated onto 6-well plates and cultured for 24 or 48 hrs. Cells were lysed in buffer containing 50 mM Tris-HCl (pH 8.0), 150 mM NaCl, 4 mM EDTA, 1% NP-40, 0.1% sodium dodecyl sulfate (SDS), 1 mM dithiothreitol (DTT) and 1 mM phenylmethylsulfonyl fluoride (PMSF). Supernatants from these lysates were subjected to SDS-polyacrylamide gel electrophoresis, followed by immunoblot analysis using anti-TSG101 antibody (BD Transduction Laboratories, San Jose, CA), anti-Alix antibody, anti-Vps4B antibody (Abnova, Taipei, Taiwan) (A302-078A; Bethyl Laboratories, Montgomery, TX), anti-CHMP4B antibody (sc-82557; Santa Cruz Biotechnology, Santa Cruz, CA), anti-HCV Core antibody, anti-β-actin antibody (Sigma), anti-Myc-Tag antibody, anti-FLAG antibody (M2; Sigma), anti-Chk2 antibody (DCS-273; MBL), anti-heat shock protein (HSP) 70 antibody (BD), Living Colors A.v. monoclonal antibody (JL-8; Clontech, Mountain View, CA), anti-HCV NS5A monoclonal antibody (no. 8926; a generous gift from A Takamizawa, The Research Foundation for Microbial Diseases of Osaka University, Japan), or anti-HCV NS5A polyclonal antibody (a generous gift from K Shimotohno, Chiba Institute of Technology, Chiba, Japan).

Immunoprecipitation Analysis

Cells were lysed in buffer containing 10 mM Tris-HCl (pH 8.0), 150 mM NaCl, 1% NP-40, 1 mM PMSF, and protease inhibitor cocktail containing 104 μM 4-(2-aminoethyl)benzenesulfonyl fluoride hydrochloride, 80 nM aprotinin, 2.1 μM leupeptin, 3.6 μM bestatin, 1.5 μM pepstatin A, and 1.4 μM E-64 (Sigma). Lysates were pre-cleaned with 30 μl of protein-G-Sepharose (GE Healthcare Bio-Sciences). Pre-cleaned supernatants were incubated with 5 μl of Living Colors A.v. monoclonal antibody or anti-FLAG antibody at 4°C for 1 hr. Following absorption of the precipitates on 30 μl of protein-G-Sepharose resin for 1 hr, the resin was washed four times with 700 μl lysis buffer. Proteins were eluted by boiling the resin for 5 min in 1× Laemmli sample buffer. The proteins were then subjected to SDS-PAGE, followed by immunoblotting analysis using either anti-FLAG antibody, Living Colors A.v. monoclonal antibody or anti-HCV Core antibody.

Statistical Analysis

Statistical comparison of the infectivity of HCV in the culture supernatants between the knockdown cells and the control cells was performed using the Student's *t*-test. *P* values of less than 0.05 were considered statistically significant. All error bars indicate standard deviation.

Results

The ESCRT system is required for HCV production

To investigate the potential role(s) of the ESCRT system in the HCV life cycle, we first used lentiviral vector-mediated RNA interference to stably knockdown the ESCRT components, including TSG101, Alix, Vps4B, or CHMP4b in HuH-7-derived RSc cured cells that cell-culture-generated HCVcc (HCV-JFH1, genotype 2a) [13] could infect and effectively replicate [14–16]. We used puromycin-resistant pooled cells 10 days after the lentiviral transduction in all experiments. Western blot and real-time LightCycler RT-PCR analyses for TSG101, Alix, Vps4B, or CHMP4b demonstrated a very effective knockdown of each ESCRT component in RSc cells transduced with lentiviral vectors expressing the corresponding shRNAs (Fig. 1A–E). Importantly, we noticed that the depletion of ESCRT components did not affect the levels of several cellular proteins, including HSP70, Chk2, and b-actin (Fig. 1A). To test the cell toxicity of each shRNA, we examined colorimetric MTT assay. In this context, we demonstrated that the shRNAs did not affect the cell viabilities (Fig. 1F). We next examined the levels of HCV Core and the infectivity of HCV in the culture supernatants as well as the level of HCV RNA in the TSG101, Alix, Vps4B, or CHMP4b stable knockdown RSc cells 97 h after HCV-JFH1 infection at an MOI of 0.1. The results showed that the release of HCV Core into the culture supernatants

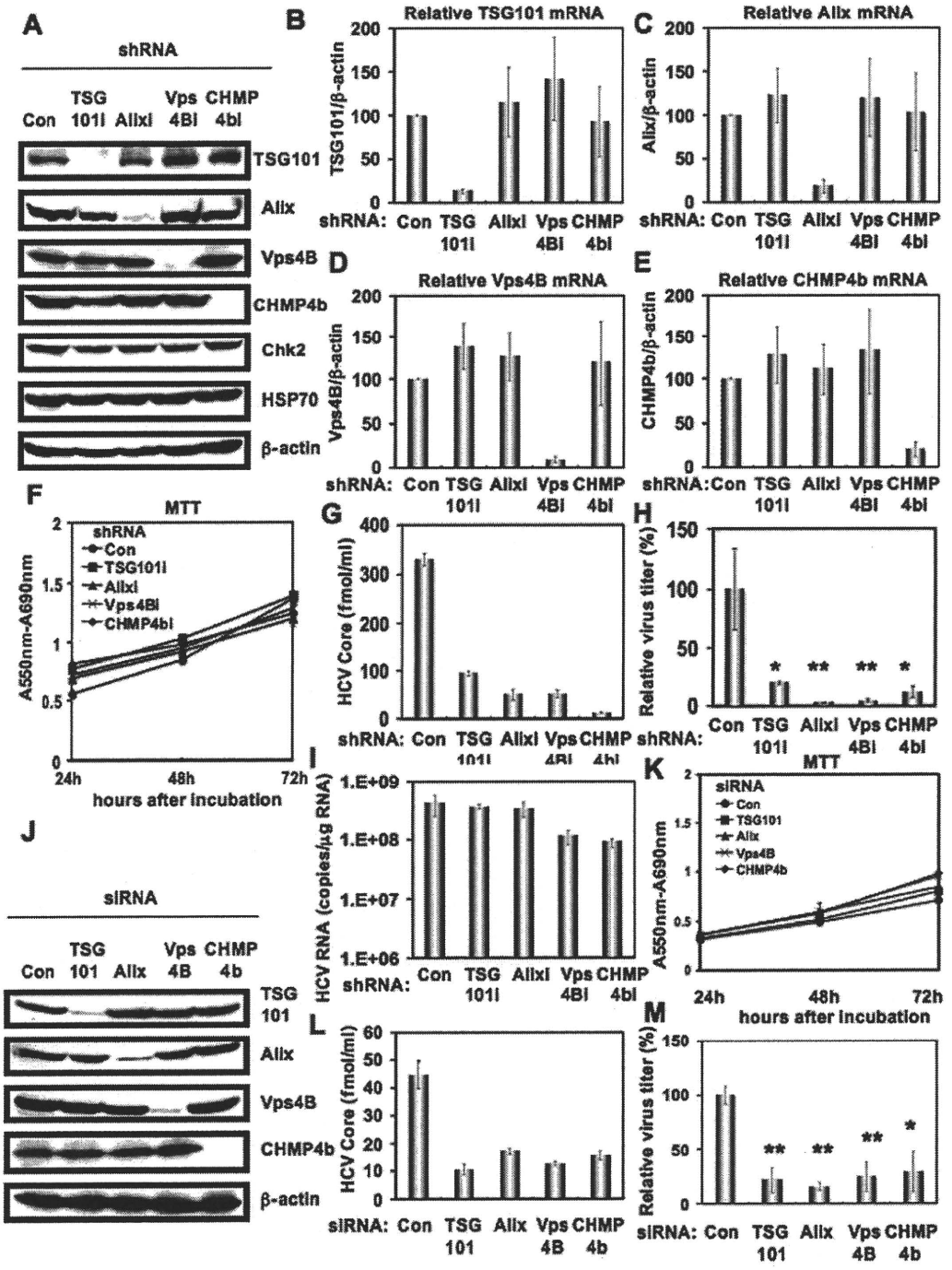

Figure 1. ESCRT components are required for the infectious HCV production. (A) Inhibition of TSG101, Alix, Vps4B, or CHMP4b protein expression by shRNA-producing lentiviral vectors. The results of the Western blot analysis of cellular lysates with anti-TSG101, anti-Alix, anti-Vps4B, anti-CHMP4b, anti-Chk2, anti-HSP70, or anti-β-actin antibody in RSc cells expressing shRNA targeted to TSG101 (TSG101i), Alix (Alixi), Vps4B (Vps4Bi), or CHMP4b (CHMP4bi) as well as in RSc cells transduced with a control lentiviral vector (Con) are shown. Real-time LightCycler RT-PCR for TSG101 (B), Alix (C), Vps4B (D), or CHMP4b mRNA (E) was performed as well as for β-actin mRNA in triplicate. Each mRNA level was calculated relative to the level in RSc cells transduced with a control lentiviral vector (Con) which was assigned as 100%. Error bars in this panel and other figures indicate standard deviations. (F) MTT assay of each knockdown RSc cells at the indicated time. (G) The levels of HCV Core in the culture supernatants from the stable knockdown RSc cells 97 h after inoculation of HCV-JFH1 at an MOI of 0.1 were determined by ELISA. Experiments were done in triplicate and columns represent the mean Core protein levels. (H) The infectivity of HCV in the culture supernatants from the stable knockdown RSc cells 97 hrs after inoculation of HCV-JFH1 at an MOI of 0.1 was determined by a focus-forming assay at 48 hrs post-infection. Experiments were done in triplicate and each virus titer was calculated relative to the level in RSc cells transduced with a control lentiviral vector (Con) which was assigned as 100%. Asterisks indicate significant differences compared to the control treatment. *$P<0.05$; **$P<0.01$. (I) The level of intracellular genome-length HCV-JFH1 RNA in the cells at 97 hrs post-infection was monitored by real-time LightCycler RT-PCR. Results

from three independent experiments are shown. (J) Inhibition of TSG101, Alix, Vps4B, or CHMP4b protein expression by 72 hrs after transient transfection of RSc cells with a pool of control siRNA (Con) or a pool of siRNA specific for Alix, Vps4B, or CHMP4b (50 nM). The results of the Western blot analysis of cellular lysates with anti-TSG101, anti-Alix, anti-Vps4B, anti-CHMP4b, or anti-β-actin antibody is shown. (K) MTT assay of each knockdown RSc cells at the indicated time. (L) The levels of HCV Core in the culture supernatants were determined by ELISA 24 hrs after inoculation of HCV-JFH1. RSc cells were transiently transfected with a pool of control siRNA (Con) or a pool of siRNA specific for TSG101, Alix, Vps4B, or CHMP4b (50 nM). At 48 hrs after transfection, the cells were inoculated with HCV-JFH1 at an MOI of 5 and incubated for 2 hrs. Then, culture medium was changed and incubated for 22 hrs. Experiments were done in triplicate and each Core level was calculated relative to the level in the culture supernatants from the control cells and indicated below. (M) The infectivity of HCV in the culture supernatants from the transient knockdown RSc cells 24 hrs after inoculation of HCV-JFH1 at an MOI of 5 was determined by a focus-forming assay at 48 hrs post-infection. Experiments were done in triplicate and each virus titer was calculated relative to the level in RSc cells transfected with a control siRNA (Con) which was assigned as 100%. Asterisks indicate significant differences compared to the control treatment. *$P<0.05$; **$P<0.01$.

doi:10.1371/journal.pone.0014517.g001

was significantly suppressed in these knockdown cells after HCV-JFH1 infection (Fig. 1G). Importantly, the infectivity of HCV in the culture supernatants was also significantly suppressed in these knockdown cells (Fig. 1H), while the RNA replication of HCV-JFH1 was not affected in the TSG101 or Alix knockdown cells and was somewhat decreased in the Vps4B and CHMP4b knockdown cells (Fig. 1I). This suggested that the ESCRT system is associated with infectious HCV production. To further confirm whether or not the ESCRT system is involved in HCV production, we analyzed the single-round HCV replication. For this, we used RSc cells transiently transfected with a pool of siRNAs specific for TSG101, Alix, Vps4B, or CHMP4b as well as a pool of control siRNAs (Con) following HCV infection. In spite of very effective knockdown of each ESCRT component (Fig. 1J), we demonstrated that the siRNAs did not affect the cell viabilities by MTT assay (Fig. 1K). Consistent with our finding using the stable knockdown cells, we observed that the release of HCV Core or the infectivity of HCV into the culture supernatants was significantly suppressed in these transient knockdown cells 24 hrs after HCV-JFH1 infection (Fig. 1L and 1M). Furthermore, we examined the effect of siRNA specific for TSG101, Alix, Vps4B, or CHMP4b in HCV RNA replication using the subgenomic JFH1 replicon, JRN/3-5B, encoding *Renilla* luciferase gene for monitoring the HCV RNA replication in HuH-7-derived OR6c JRN/3-5B cells (Fig. 2A and 2B) or an OR6 assay system, which was developed as a luciferase reporter assay system for monitoring genome-length HCV RNA replication (HCV-O, genotype 1b) in HuH-7-derived OR6 cells (Fig. 2C) [17,18]. The results showed that these siRNAs could not affect HCV RNA replication as well as the levels of intracellular NS5A proteins (Fig. 2A–C). Although we have demonstrated that the ESCRT system is required for production of extracellular infectious HCV particles, it is not clear whether or not these findings are associated with the assembly of intracellular infectious particles. To test this point, infectivity of intracellular infectious particles was analyzed following lysis of HCV-JFH1-infected knockdown cells by repetitive freeze and thaw. Consequently, we did not observe any significant effects of siRNAs on the accumulation of intracellular infectious HCV-JFH1, while the accumulation of extracellular HCV was significantly suppressed in these knockdown cells (Fig. 2D and 2E), indicating that inhibition of the ESCRT system does not block the accumulation of intracellular infectious HCV particles. Furthermore, Western blot analysis of cell lysates demonstrated that the level of intracellular HCV Core and NS5A was not affected in these knockdown cells 72 hrs post-infection (Fig. 2F). Thus, we conclude that the ESCRT system is not required for the assembly of infectious particles but the ESCRT system is required for late step of HCV production.

HCV Core can target into lipid droplets in the ESCRT knockdown cells

Since lipid droplets have been shown to be involved in an important cytoplasmic organelle for HCV production [4], we performed immunofluorescence and confocal microscopic analyses to determine whether or not HCV Core misses localization into lipid droplets in the ESCRT knockdown cells. We found that the Core was targeted into lipid droplets even in TSG101 knockdown, Alix knockdown, Vps4B knockdown, or CHMP4b knockdown RSc cells as well as in the control RSc cells after HCV infection (Fig. 3). This suggests that the ESCRT system plays a role in the late step after the Core is targeted into lipid droplets in the HCV life cycle.

HCV Core interacts with CHMP4b

To determine whether or not HCV Core can interact with ESCRT component(s), we examined their subcellular localization by confocal laser scanning microscopy. Consequently, the Core mostly colocalized with CHMP4b-green fluorescent protein (GFP) or FLAG-tagged CHMP4b in the perinuclear region of 293FT cells coexpressing them (Fig. 4A and 4B), while the CHMP4b-GFP alone was slightly diffused in the cytoplasm (Fig. 4A), indicating the recruitment of CHMP4b in the Core-expressing area. Importantly, we observed similar partial colocalization in HCV-JFH1-infected RSc cells expressing CHMP4b-GFP (Fig. 4C), whereas the CHMP4b-GFP alone was diffused in the cytoplasm in the uninfected RSc cells (Fig. 4C), suggesting the interaction of HCV Core with CHMP4b. Unfortunately, we failed to observe endogenous CHMP4b using several commercially available anti-CHMP4b antibody (data not shown). Consistent with a previous report that interaction between HCV Core and NS5A is critical for HCV production [3], we found the partial colocalization of NS5A with CHMP4b-GFP as well as the colocalization of Core with CHMP4b-GFP in HCV-JFH1-infected RSc cells (Fig. 4C). Then, we examined whether or not HCV Core can bind to CHMP4b by immunoprecipitation analysis. 293FT cells transfected with 4 mg of pCHMP4b-GFP, pEGFP C3 (Clontech), pcDNA3-FLAG [19], pcDNA3-FLAG-Alix or pFLAG-CHMP4b and RSc cells 5 days after inoculation of HCV-JFH1 at an MOI of 4 were lysed and performed immunoprecipitation of lysate mixtures of HCV-JFH1-infected RSc cells and 293FT cells expressing CHMP4b-GFP, GFP alone, FLAG-CHMP4b or FLAG-epitope alone with anti-FLAG or anti-GFP antibody. Consequently, we observed that the Core but not the NS5A could bind to FLAG-CHMP4b (Fig. 4D). However, the Core was not immunoprecipitated with anti-FLAG antibody using the lysate mixtures of HCV-JFH1-infected RSc cell lysates and 293FT cells expressing FLAG-epitope alone or FLAG-Alix (Fig. 4D). Furthermore, the Core was coimmunoprecipitated with CHMP4b-GFP but not GFP when lysate mixtures of HCV-JFH1-infected RSc cells and 293FT cells expressing CHMP4b-GFP or GFP alone were used (Fig. 4D). In contrast, we failed to observe the marked colocalization of HCV-JFH1 Core with Myc-tagged TSG101 in HCV-JFH1-infected RSc cells expressing Myc-TSG101 or endogenous Alix in HCV-JFH1-infected RSc cells (Fig. 5A). Thus, we concluded that the HCV Core was associated with CHMP4b.

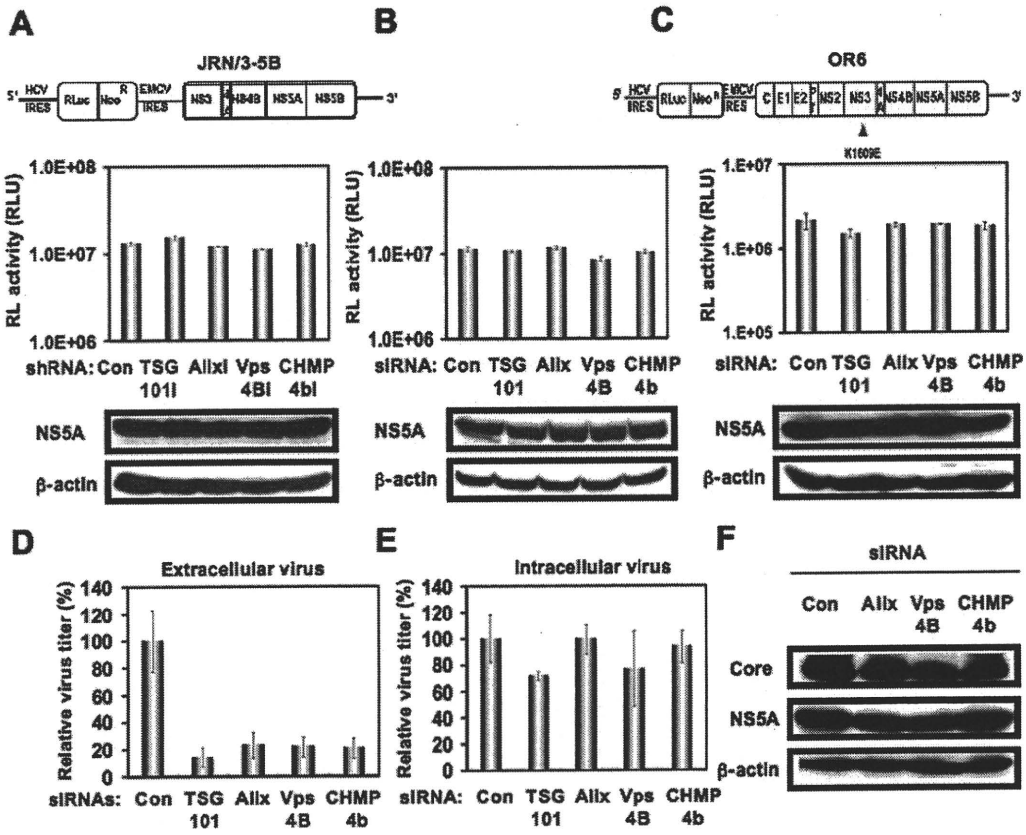

Figure 2. ESCRT system is not required for HCV RNA replication and assembly of intracellular infectious HCV. (A) Schematic gene organization of subgenomic JFH1 (JRN/3-5B) RNA encoding *Renilla* luciferase gene. Renilla luciferase gene (RLuc) is depicted as a box and is expressed as a fusion protein with Neo. The HCV RNA replication level in each ESCRT knockdown OR6c JRN/3-5B cells by lentiviral vector-mediated RNA interference (shRNA) was monitored by RL assay. The RL activity (RLU) is shown. The results shown are means from three independent experiments. (B) 72 hrs after the transfection of OR6c JRN/3-5B polyclonal cells with each of the siRNA (50 nM), the HCV RNA replication level was monitored by RL assay as described in (A). (C) Schematic gene organization of genome-length HCV-O RNA encoding *Renilla* luciferase gene. The position of an adaptive mutation, K1609E, is indicated by a triangle. 72 hrs after the transfection of OR6 cells with each of the siRNA (50 nM), the HCV RNA replication level was monitored by RL assay as described in (A). (D) The infectivity of HCV in the culture supernatants from the transient knockdown RSc cells 24 hrs after inoculation of HCV-JFH1 at an MOI of 2 was determined by a focus-forming assay at 48 hrs post-infection. Experiments were done in triplicate and each virus titer was calculated relative to the level in RSc cells transfected with a control siRNA (Con) which was assigned as 100%. (E) Intracellular HCV infectivity was determined by a focus-forming assay at 48 hrs post-inoculation of lysates by repeated freeze and thaw cycles as described in (D). (F) RSc cells were transiently transfected with a pool of control siRNA (Con) or a pool of siRNA specific for Alix, Vps4B, or CHMP4b (50 nM). At 24 hrs after the transfection, the cells were inoculated with HCV-JFH1 at an MOI of 0.2 and incubated for 48 hrs. Then, culture medium was changed and incubated for 24 hours. Western blotting of cell lysates 72 hrs post-infection with anti-β-actin, anti-HCV NS5A, or anti-HCV Core antibody is shown.
doi:10.1371/journal.pone.0014517.g002

Finally, we examined the subcellular localization of HCV Core and Brox, a novel farnesylated Bro1 domain-containing protein, since Brox was recently identified as a CHMP4-binding protein [27]. In this context, the Core partially colocalized with GFP-Brox in 293FT cells coexpressing of HCV Core and GFP-Brox (Fig. 5B). Importantly, we observed similar partial colocalization in HCV-JFH1-infected RSc cells expressing GFP-Brox (Fig. 5C). On the other hand, the CHMP4b-GFP alone was diffused in the cytoplasm of uninfected RSc cells (Fig. 5C). To examine the potential role of Brox in HCV life cycle, we established the Brox knockdown RSc cells by lentiviral vector expressing shRNA targeted to Brox (Fig. 5D). Consequently, we found that the release of HCV Core or the infectivity of HCV into the culture supernatants was significantly suppressed in the Brox knockdown cells 4 days after HCV-JFH1 infection (Fig. 5E and 5F), while the RNA replication of HCV-JFH1 was marginally affected in the knockdown cells (Fig. 5G) in spite of the very effective knockdown of Brox mRNA (Fig. 5D), suggesting that Brox is also required for the infectious HCV production.

Discussion

In this study, we have demonstrated that the ESCRT system is required for infectious HCV production, and that HCV Core but not NS5A binds to CHMP4b, a component of ESCRT-III. Although RNA replication of HCV-JFH1 was not affected in the TSG101 knockdown or the Alix knockdown cells, the infectivity of HCV in the culture supernatants was significantly suppressed in these knockdown cells after HCV-JFH1 infection (Fig. 1G and 1H). Furthermore, siRNA targeted to TSG101, Alix, Vps4B, or CHMP4b significantly suppressed HCV Core level or the infectivity of HCV in the culture supernatants (Fig. 1L, 1M, and

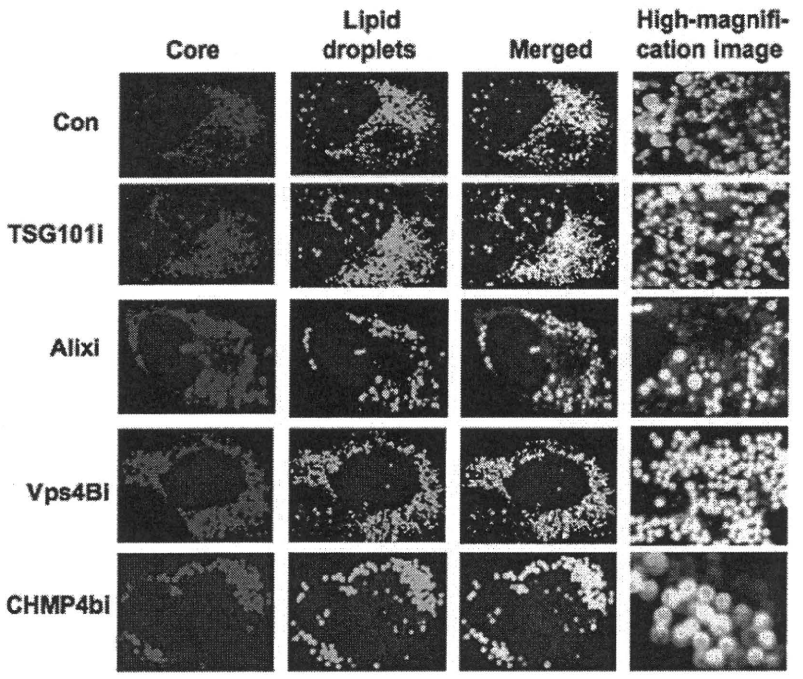

Figure 3. HCV Core is targeted to lipid droplets even in the ESCRT knockdown cells. The RSc cells transduced with a control lentiviral vector (Con), the TSG101 knockdown (TSG101i), the Alix knockdown (Alixi), the Vps4B knockdown (Vps4Bi), or the CHMP4b knockdown (CHMP4bi) cells were infected with HCV-JFH1. Cells were fixed 60 hrs post-infection and were then examined by confocal laser scanning microscopy. Cells were stained with anti-HCV Core (CP-9 and CP-11 mixture) and were then visualized with Cy3 (red). Lipid droplets and nuclei were stained with BODIPY 493/503 (green) and DAPI (blue), respectively. Images were visualized using confocal laser scanning microscopy. Colocalization is shown in yellow (Merged).
doi:10.1371/journal.pone.0014517.g003

2D), while the siRNA did not affect intracellular HCV Core level (Fig. 2E and 2F). Accordingly, we noticed some discrepancy that shRNA targeted to Vps4B or CHMP4b somewhat decreased intracellular HCV RNA replication (Fig. 1I), whereas siRNA targeted to TASG101, Alix, Vps4B or CHMP4b did not affect the RNA replication of subgenomic replicon of JFH1 (Fig. 2A and 2B). Furthermore, siRNAs targeted to TSG101, Alix, Vps4B, or CHMP4b did not affect HCV-O (genotype 1b) RNA replication using the OR6 assay system [17,18] (Fig. 2C), indicating that the ESCRT system is unrelated to the HCV RNA replication of genotype 1b. Thus, we suggested that the ESCRT system is not significant for HCV RNA replication. Within the family *Flaviviridae*, NS3 of the Japanese encephalitis virus (JEV) is also known to interact with TSG101 and microtubules, suggesting their potential roles in JEV assembly [28]. Accordingly, HCV NS3 has been involved in HCV particle assembly and infectivity [29,30]. However, whether HCV NS3 or another HCV protein binds to TSG101 remains to be investigated. At least, we did not observe the interaction between HCV NS5A and CHMP4b (Fig. 4D), Alix (Fig. 4D), TSG101, or Vps4B (data not shown).

Efficient enveloped virus release requires *cis*-acting viral late domains (L-domains), including P(T/S)AP, YPXnL (where X is any amino acid), and PPXY amino acid L-domain motif that are found in the structural proteins of other enveloped viruses [10,11]. Unlike the case with these enveloped viruses, we failed to find the three types of conserved viral L-domain motif in the HCV-JFH1 Core (data not shown). Nevertheless, we observed that the Core bound to CHMP4b, whereas NS5A did not (Fig. 4D), suggesting that the Core has a novel motif required for the HCV production. In this regard, Blanchard *et al.* reported that the aspartic acid at position 111 in the Core is crucial for virus assembly [31]. Interestingly, the conversion of the aspartic acid into alanine at amino acid 111 (PTDP to PTAP), which creates the PTAP L-domain motif, enhanced the release of HCV Core in the cell culture medium (a 2.5-fold increase) compared with the wild-type Core [31]. In contrast, Klein *et al.* demonstrated that the D111A mutation in the Core had no effect on HCV capsid assembly [32]. Furthermore, Murray *et al* found that serine 99, a putative phosphorylation site, in the Core was essential for infectious virion production [7]. In any event, the Core motif that is needed for interaction with the ESCRT components remains to be identified.

Ubiquitin modification of viral protein has been implicated in virion egress as well as in protein turnover. Indeed, the ubiquitin/proteasome system is required for the retrovirus budding machinery, since proteasome inhibition interferes with retroviral Gag polyprotein processing, release, and maturation. The ubiquitin modification of the HIV-1 p6 domain of Gag enhances TSG101 binding [12]. In the case of HCV Core, proteasomal degradation of the Core is mediated by two distinct mechanisms [33–36]. E6AP E3 ubiquitin ligase mediates ubiquitylation and degradation of the Core [34]. In contrast, proteasome activator PA28γ (11S regulator γ), an HCV Core-binding protein, is involved in the ubiquitin-independent degradation of the Core and HCV propagation [33,35,36]. However, little is known whether or not the ubiquitin modification of the Core might be involved in HCV egress like other enveloped viruses.

Finally, the identification of the site of viral particle assembly and budding is an intriguing issue. In case of HCV, at present, it is very difficult to visualize the HCV budding site in the infected cells by an electron microscopy. However, recent studies suggested that lipid droplets are an important cytoplasmic organelle for HCV production [4]. In this regard, Shavinskaya *et al.* demonstrated that

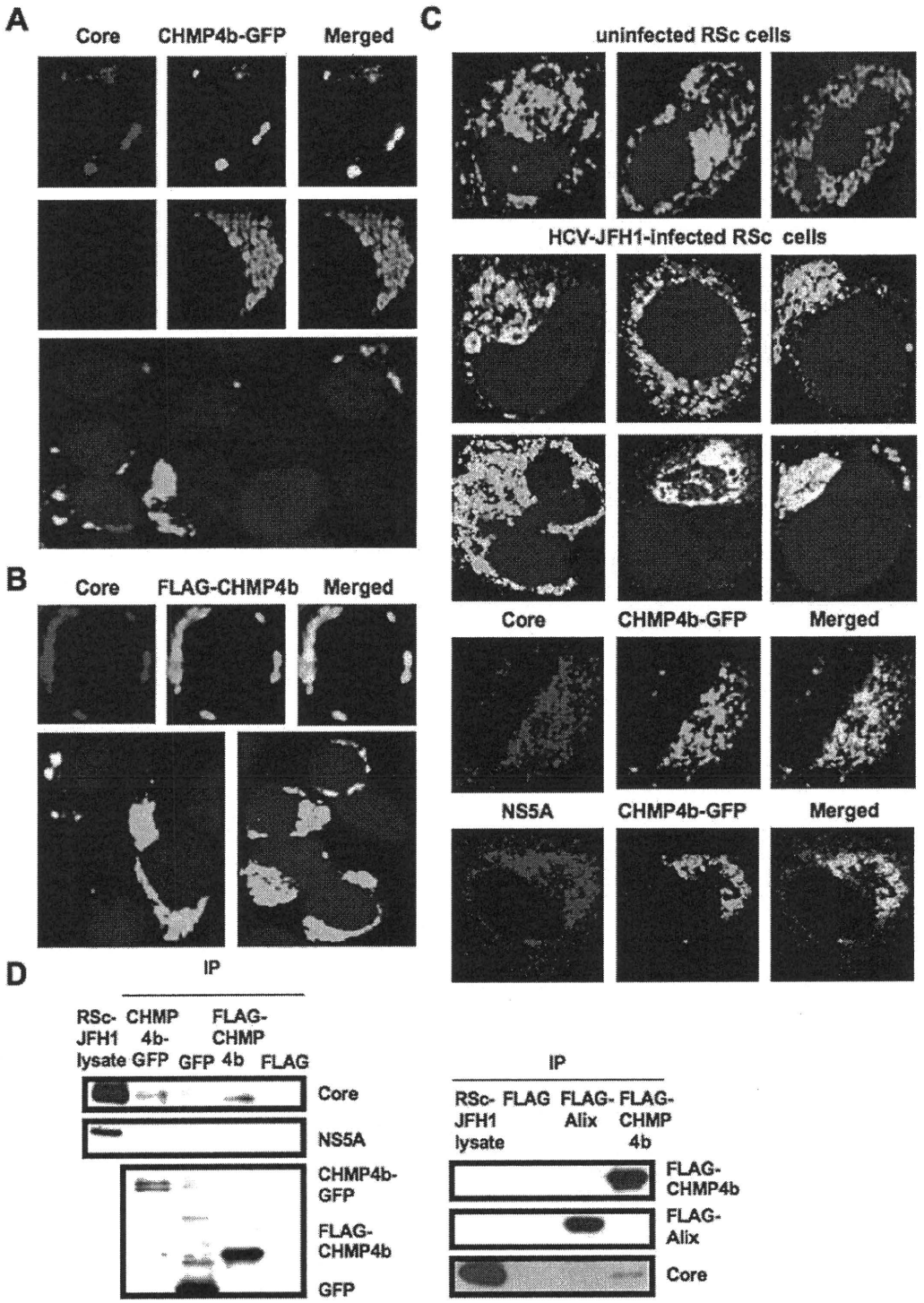

Figure 4. HCV Core interacts with CHMP4b. (A–C) HCV Core colocalizes with CHMP4b. 293FT cells cotransfected with 100 ng of pcDNA3/core (JFH1) and either 100 ng of pCHMP4b-GFP [39] (A) or pFLAG-CHMP4b [39] (B) were examined by confocal laser scanning microscopy. Cells were stained with anti-HCV Core and anti-FLAG polyclonal antibody and were then visualized with FITC (FLAG-CHMP4b) or Cy3 (Core). Images were visualized using confocal laser scanning microscopy. The right panels exhibit the two-color overlay images (Merged). Colocalization is shown in yellow. (C) The Core or NS5A partially colocalizes with CHMP4b in HCV-JFH1-infected RSc cells. RSc cells transfected with 100 ng of pCHMP4b-GFP were infected with HCV-JFH1. Cells were fixed 60 hrs post-infection and were then examined by confocal laser scanning microscopy as shown in panel (A). (D) HCV Core binds to CHMP4b. 293FT cells transfected with 4 μg of pCHMP4b-GFP, pEGFP C3 (Clontech), pcDNA3-FLAG, pcDNA3-FLAG-Alix or pFLAG-CHMP4b and RSc cells 5 days after inoculation of HCV-JFH1 at an MOI of 4 were lysed. The mixtures of these lysates were immunoprecipitated with either anti-FLAG or Living Colors A.v. monoclonal antibody (anti-GFP antibody), followed by immunoblot analysis using anti-HCV Core, anti-HCV NS5A, anti-FLAG, and/or Living Colors A.v. monoclonal antibody.
doi:10.1371/journal.pone.0014517.g004

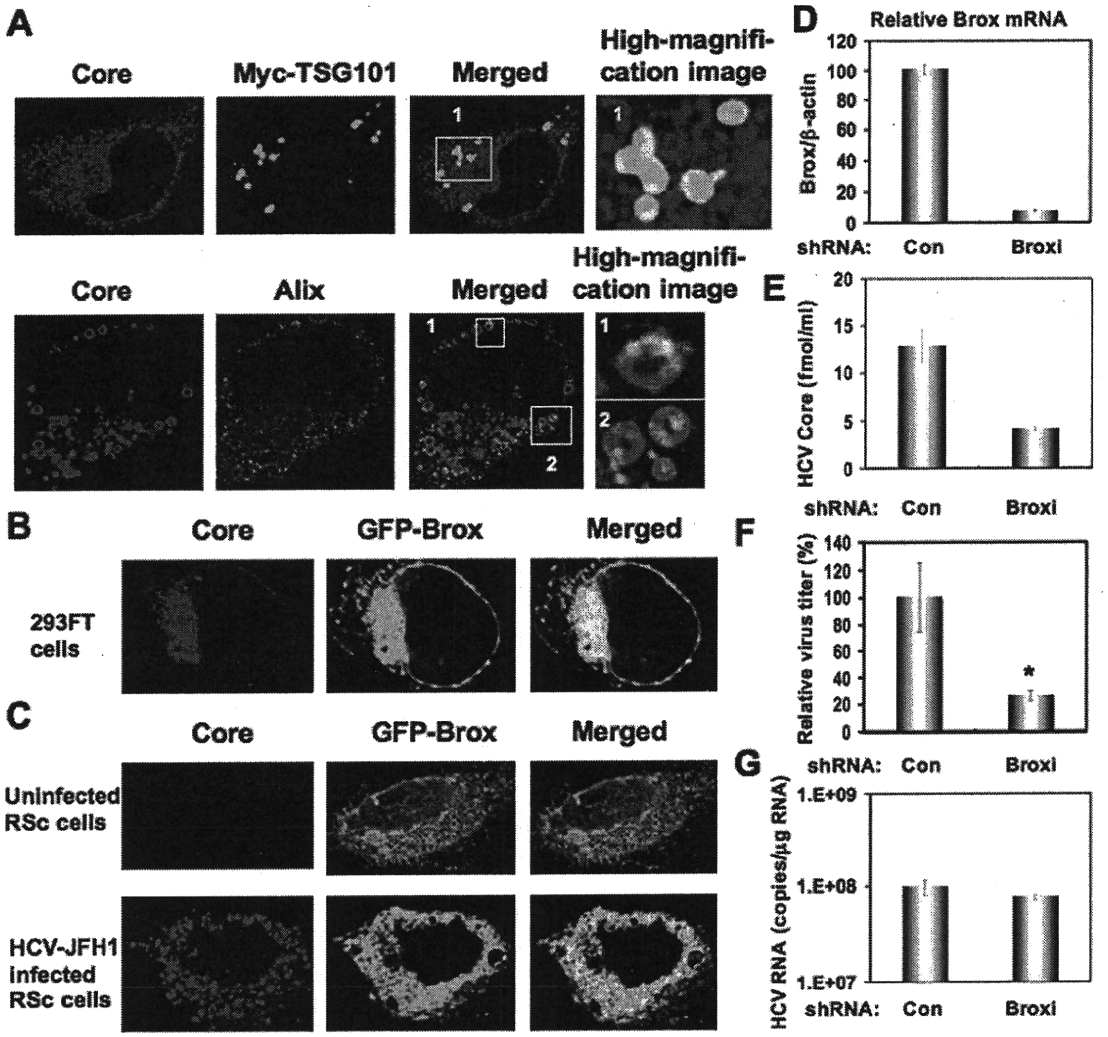

Figure 5. Brox is required for HCV life cycle. (A) Subcellular localization of Myc-tagged TSG101 in HCV-JFH1-infected RSc cells. RSc cells transfected with 100 ng of pBj-Myc-TSG101 [40] were infected with HCV-JFH1. Cells were fixed 60 hrs post-infection and were then examined by confocal laser scanning microscopy as shown in Fig. 3. High magnification image of area 1 is shown. Subcellular localization of endogenous Alix in HCV-JFH1-infected RSc cells 60 hrs post-infection. Cells were stained with anti-Alix and anti-HCV Core antibodies and were examined by confocal laser scanning microscopy. High magnification images of area 1 and area 2 are shown. (B) HCV Core partially colocalizes with Brox. 293FT cells cotransfected with 100 ng of pcDNA3/core (JFH1) and 100 ng of pmGFP-Brox^{WT} [27] were examined by confocal laser scanning microscopy. (C) The HCV Core partially colocalizes with Brox in HCV-JFH1-infected RSc cells. RSc cells transfected with 100 ng of pmGFP-Brox^{WT} were infected with HCV-JFH1. Cells were fixed 60 hrs post-infection and were then examined by confocal laser scanning microscopy. (D) Inhibition of Brox mRNA expression by the shRNA-producing lentiviral vector. Real-time LightCycler RT-PCR for Brox was performed as well as for β-actin mRNA in triplicate. Each mRNA level was calculated relative to the level in RSc cells transduced with a control lentiviral vector (Con) which was assigned as 100%. (E) The levels of HCV Core in the culture supernatants from the Brox knockdown RSc cells (Broxi) 72 hrs after inoculation of HCV-JFH1 were determined by ELISA. (F) The infectivity of HCV in the culture supernatants was determined by a focus-forming assay at 48 hrs post-infection. Experiments were done in triplicate and each virus titer was calculated relative to the level in RSc cells transduced with a control lentiviral vector (Con) which was assigned as 100%. Asterisks indicate significant differences compared to the control treatment. *$P<0.05$; **$P<0.01$. (G) The levels of intracellular genome-length HCV-JFH1 RNA in the cells used in (E) were monitored by real-time LightCycler RT-PCR.
doi:10.1371/journal.pone.0014517.g005

the lipid droplet-binding domain of the Core is a major determinant for efficient virus assembly [6]. The HCV Core induces lipid droplet redistribution in a microtubule- and dynein-dependent manner, since disrupting the microtubule network reduced the HCV titer, implicating transport networks in virus assembly and release [2]. Furthermore, Sandrin *et al.* reported that HCV envelope proteins localized to ESCRT-associated multivesicular body (MVB) [37]. Quite recently, Corless *et al.* have demonstrated that Vps4B and the ESCRT-III complex are required for HCV production [38]. Consistent with our findings, their dominant-negative forms of Vps4B and CHMP4B clearly suppressed HCV production. However, their dominant-negative forms of TSG101 and Alix failed to suppress the HCV production and they suggested that both TSG101 and Alix are unrelated to the HCV production. In contrast, we have demonstrated both TSG101 and Alix are also required for the infectious HCV

production by using shRNAs and siRNAs (Fig. 1). We may partly explain such discrepancy due to the difference of the methodology in our study utilized shRNAs and siRNAs instead of dominant-negative forms of TSG101 and Alix. Importantly, they demonstrated that the dominant-negative forms of Vps4B and CHMP4b did not affect the HCV RNA replication and the accumulation of intracellular infectious particles, suggesting that Vps4B and CHMP4b are unrelated to HCV RNA replication. Indeed, we have demonstrated that the ESCRT system is not required for the assembly of intracellular infectious HCV particles (Fig. 2E). Notably, we have demonstrated for the first time that HCV Core associated with CHMP4b (Fig. 4). Accordingly, we have also demonstrated that Brox, a CHMP4b binding protein, is required for HCV production (Fig. 5D–G). Taking together the past and present findings, we propose that the ESCRT system is involved in infectious HCV production after the HCV assembly that occurs on lipid droplets.

Acknowledgments

We thank D. Trono, R. Iggo, R. Agami, A. Takamizawa, and K. Shimotohno for pCMVΔR8.91, pMDG2, pSUPER, pRDI292, and anti-NS5A antibody, respectively. We also thank K. Abe for construction of pJRN/3-5B and T. Nakamura for his technical assistance.

Author Contributions

Conceived and designed the experiments: YA NK. Performed the experiments: YA MK. Analyzed the data: YA. Contributed reagents/materials/analysis tools: MM MI HD TW. Wrote the paper: YA NK.

References

1. Kato N, Hijikata M, Ootsuyama Y, Nakagawa M, Ohkoshi S, et al. (1990) Molecular cloning of the human hepatitis C virus genome from Japanese patients with non-A, non-B hepatitis. Proc Natl Acad Sci USA 87: 9524–9528.
2. Boulant S, Douglas MW, Moody L, Budkowska A, Targett-Adams P, et al. (2008) Hepatitis C virus core protein induces lipid droplet redistribution in a microtubule- and dynein-dependent manner. Traffic 9: 1268–1282.
3. Masaki T, Suzuki R, Murakami K, Aizaki H, Ishii K, et al. (2008) Interaction of hepatitis C virus nonstructural protein 5A with core protein is critical for the production of infectious virus particles. J Virol 82: 7964–7976.
4. Miyanari Y, Atsuzawa K, Usuda N, Watashi K, Hishiki T, et al. (2007) The lipid droplet is an important organelle for hepatitis C virus production. Nat Cell Biol 9: 1089–1097.
5. Shi ST, Polyak SJ, Tu H, Taylor DR, Gretch DR, et al. (2002) Hepatitis C virus NS5A colocalizes with the core protein on lipid droplets and interacts with apolipoproteins. Virology 292: 198–210.
6. Shavinskaya A, Boulant S, Penin F, McLauchlan J, Bartenschlager R (2007) The lipid droplet binding domain of hepatitis C virus core protein is a major determinant for efficient virus assembly. J Biol Chem 282: 37158–37169.
7. Murray CL, Jones CT, Tassello J, Rice CM (2007) Alanine scanning of the hepatitis C virus core protein reveals numerous residues essential for production of infectious virus. J Virol 81: 10220–10231.
8. Appel N, Zayas M, Miller S, Krijnse-Locker J, Schaller T, et al. (2008) Essential role of domain III of nonstructural protein 5A for hepatitis C virus infectious particle assembly. PLOS Pathog 4: e1000035.
9. Tellinghuisen TL, Foss KL, Treadaway J (2008) Regulation of hepatitis C virion production via phosphorylation of the NS5A protein. PLoS Pathog 4: e1000032.
10. Bieniasz PD (2006) Late budding domains and host proteins in enveloped virus release. Virology 344: 55–63.
11. Chen BJ, Lamb RA (2008) Mechanisms for enveloped virus budding: Can some viruses do without an ESCRT? Virology 372: 221–232.
12. Garrus JE, von Schwedler UK, Pornillos OW, Morham SG, Zavitz KH, et al. (2001) Tsg101 and vacuolar protein sorting pathway are essential for HIV-1 budding. Cell 107: 55–65.
13. Wakita T, Pietschmann T, Kato T, Date T, Miyamoto M, et al. (2005) Production of infectious hepatitis C virus in tissue culture from a cloned viral genome. Nat Med 11: 791–796.
14. Ariumi Y, Kuroki M, Abe K, Dansako H, Ikeda M, et al. (2007) DDX3 DEAD-box RNA helicase is required for hepatitis C virus RNA replication. J Virol 81: 13922–13926.
15. Ariumi Y, Kuroki M, Dansako H, Abe K, Ikeda M, et al. (2008) The DNA damage sensors, ataxia-telangiectasia mutated kinase and checkpoint kinase 2 are required for hepatitis C virus RNA replication. J Virol 82: 9639–9646.
16. Kuroki M, Ariumi Y, Ikeda M, Dansako H, Wakita T, et al. (2009) Arsenic trioxide inhibits hepatitis C virus RNA replication through modulation of the glutathione redox system and oxidative stress. J Virol 83: 2338–2348.
17. Ikeda M, Abe K, Dansako H, Nakamura T, Naka K, et al. (2005) Efficient replication of a full-length hepatitis C virus genome, strain O, in cell culture, and development of a luciferase reporter system. Biochem Biophys Res Commun 329: 1350–1359.
18. Ikeda M, Abe K, Yamada M, Dansako H, Naka K, et al. (2006) Different anti-HCV profiles of statins and their potential combination therapy with interferon. Hepatology 44: 117–125.
19. Ariumi Y, Kaida A, Hatanaka M, Shimotohno K (2001) Functional cross-talk of HIV-1 Tat with p53 through its C-terminal domain. Biochem Biophys Res Commun 287: 556–561.
20. Abe K, Ikeda M, Ariumi Y, Dansako H, Wakita T, et al. (2009) HCV genotype 1b chimeric replicon with NS5B of JFH-1 exhibited resistance to cyclosporine A. Arch Virol 154: 1671–1677.
21. Ariumi Y, Ego T, Kaida A, Matsumoto M, Pandolfi PP, et al. (2003) Distinct nuclear body components, PML and SMRT, regulate the trans-acting function of HTLV-1 Tax oncoprotein. Oncogene 22: 1611–1619.
22. Brummelkamp TR, Bernard R, Agami R (2002) A system for stable expression of short interfering RNAs in mammalian cells. Science 296: 550–553.
23. Bridge AJ, Pebernard S, Ducraux A, Nicoulaz AL, Iggo R (2003) Induction of an interferon response by RNAi vectors in mammalian cells. Nat Genet 34: 263–264.
24. Ariumi Y, Priscilla T, Masutani M, Trono D (2005) DNA damage sensors ATM, ATR, DNA-PKcs, and PARP-1 are dispensable for human immunodeficiency virus type 1 integration. J Virol 79: 2973–2978.
25. Naldini L, Blömer U, Gallay P, Ory D, Mulligan R, et al. (1996) In vivo gene delivery and stable transduction of non-dividing cells by a lentiviral vector. Science 272: 263–267.
26. Zufferey R, Nagy D, Mandel RJ, Naldini L, Trono D (1997) Multiply attenuated lentiviral vector achieves efficient gene delivery in vivo. Nat Biotechnol 15: 871–875.
27. Ichioka F, Kobayashi R, Katoh K, Shibata H, Maki M (2008) Brox, a novel farnesylated Brol domain-containing protein that associates with charged multivesicular body protein 4 (CHMP4). FEBS J 275: 682–692.
28. Chiou CT, Hu CCA, Chen PH, Liao CL, Lin YL, et al. (2003) Association of Japanese encephalitis virus NS3 protein with microtubules and tumor susceptibility gene 101 (TSG101) protein. J Gen Virol 84: 2795–2805.
29. Yi M, Ma Y, Yates J, Lemon SM (2007) Compensatory mutations in E1, p7, NS2, and NS3 enhance yields of cell culture-infectious intergenotypic chimeric hepatitis C virus. J Virol 81: 629–638.
30. Ma Y, Yates J, Liang Y, Lemon SM, Yi M (2008) NS3 helicase domains involved in infectious intracellular hepatitis C virus particle assembly. J Virol 82: 7624–7639.
31. Blanchard E, Hourioux C, Brand D, Ait-Goughoulte M, Moreau A, et al. (2003) Hepatitis C virus-like particle budding: Role of the core protein and importance of its Asp^{111}. J Virol 77: 10131–10138.
32. Klein KC, Dellos SR, Lingappa JR (2005) Identification of residues in hepatitis C virus core protein that are critical for capsid assembly in a cell-free system. J Virol 79: 6814–6826.
33. Moriishi K, Okabayashi T, Nakai K, Moriya K, Koike K, et al. (2003) Proteasome activator 28γ-dependent nuclear retention and degradation of hepatitis C virus core protein. J Virol 77: 10237–10249.
34. Shirakawa M, Murakami K, Ichimura T, Suzuki R, Shimoji T, et al. (2007) E6AP ubiquitin ligase mediates ubiquitylation and degradation of hepatitis C virus core protein. J Virol 81: 1174–1185.
35. Suzuki R, Moriishi K, Fukuda K, Shirakura M, Ishii K, et al. (2009) Proteasomal turnover of hepatitis C virus core protein is regulated by two distinct mechanisms: a ubiquitin-dependent mechanism and a ubiquitin-independent but PA28γ-dependent mechanism. J Virol 83: 2389–2392.
36. Moriishi K, Shoji I, Mori R, Suzuki R, Suzuki T, et al. (2010) Involvement of PA28gamma in the propagation of hepatitis C virus. Hepatology 52: 411–420.
37. Sandrin V, Boulanger P, Penin F, Granier C, Cosset FL, et al. (2005) Assembly of functional hepatitis C virus glycoproteins on infectious pseudoparticles occurs intracellularly and requires concomitant incorporation of E1 and E2 glycoproteins. J Gen Virol 86: 3189–3199.
38. Corless L, Crump CM, Griffin SD, Harris M (2010) Vps4 and ESCRT-III complex are required for the release of infectious hepatitis C virus particles. J Gen Virol 91: 362–372.
39. Katoh K, Shibata H, Suzuki H, Nara A, Ishidoh K, et al. (2003) The ALG-2-interacting protein Alix associates with CHMP4b, a human homologue of yeast Snf7 that is involved in multivesicular body sorting. J Biol Chem 278: 39104–39113.
40. Katoh K, Suzuki H, Terasawa Y, Mizuno T, Yasuda J, et al. (2005) The penta-FF-hand protein ALG-2 interacts directly with the ESCRT-I component TSG101, and Ca^{2+}-dependently co-localizes to aberrant endosomes with dominant-negative AAA ATPase SKD1/Vps4B. Biochem J 391: 677–685.

Hepatology Research

Hepatology Research 2010; 40: 1248–1253 doi: 10.1111/j.1872-034X.2010.00730.x

Short Communication

Gene expression profile of Li23, a new human hepatoma cell line that enables robust hepatitis C virus replication: Comparison with HuH-7 and other hepatic cell lines

Kyoko Mori,* Masanori Ikeda, Yasuo Ariumi and Nobuyuki Kato*

Department of Tumor Virology, Okayama University Graduate School of Medicine, Dentistry and Pharmaceutical Sciences, Okayama, Japan

Aim: Human hepatoma cell line HuH-7-derived cells are currently the only cell culture system used for robust hepatitis C virus (HCV) replication. We recently found a new human hepatoma cell line, Li23, that enables robust HCV replication. Although both cell lines had similar liver-specific expression profiles, the overall profile of Li23 seemed to differ considerably from that of HuH-7. To understand this difference, the expression profile of Li23 cells was further characterized by a comparison with that of HuH-7 cells.

Methods: cDNA microarray analysis using Li23 and HuH-7 cells was performed. Li23-derived ORL8c cells and HuH-7-derived RSc cells, in which HCV could infect and efficiently replicate, were also used for the microarray analysis. For the comparative analysis by reverse transcription polymerase chain reaction (RT–PCR), human hepatoma cell lines (HuH-6, HepG2, HLE, HLF and PLC/PRF/5) and immortalized hepatocyte cell line (PH5CH8) were also used.

Results: Microarray analysis of Li23 versus HuH-7 cells selected 80 probes to represent highly expressed genes that have ratios of more than 30 (Li23/HuH-7) or 20 (HuH-7/Li23). Among them, 17 known genes were picked up for further analysis. The expression levels of most of these genes in Li23 and HuH-7 cells were retained in ORL8c and RSc cells, respectively. Comparative analysis by RT–PCR using several other hepatic cell lines resulted in the classification of 17 genes into three types, and identified three genes showing Li23-specific expression profiles.

Conclusion: Li23 is a new hepatoma cell line whose expression profile is distinct from those of frequently used hepatic cell lines.

Key words: hepatitis C virus, hepatoma cell line, HuH-7, Li23, microarray

INTRODUCTION

HUH-7, A HUMAN hepatoma cell line,[1] is frequently used in the research of hepatitis C virus (HCV), since an HCV replicon system enabling HCV subgenomic RNA replication was developed using HuH-7 cells.[2] Even with the use of an efficient HCV production system developed in 2005,[3] HuH-7-derived cells are still used as the only cell line for persistent HCV production systems.

Correspondence: Professor Nobuyuki Kato, Department of Tumor Virology, Okayama University Graduate School of Medicine, Dentistry and Pharmaceutical Sciences, Okayama 700-8558, Japan. Email: nkato@md.okayama-u.ac.jp

*These authors contributed equally to this work.

Received 21 July 2010; revision 16 August 2010; accepted 17 August 2010.

We previously developed HCV replicon systems[4,5] and an HCV production system[6] using HuH-7-derived cells. Furthermore, we recently found a new human hepatoma cell line, Li23, that enables robust HCV RNA replication and persistent HCV production.[7] In that study, using microarray analysis, we excluded the possibility that the obtained Li23-derived cells were derived from contamination of HuH-7-derived cells used for HCV replication.[7] In addition, we noticed that the gene expression profile of Li23 cells seemed considerably different from that of HuH-7 cells. Therefore, we assumed that the Li23 cell line possesses a unique expression profile among widely used human hepatoma cell lines. To evaluate this assumption, we further characterized the expression profile of Li23 cells by comparing it with those of other human hepatoma cell lines, including HuH-7,[1] HuH-6,[8] HepG2,[9] HLE,[10] HLF[10] and PLC/PRF/5.[11] Human immortalized hepatocyte cell line

PH5CH8[12] was also used for the comparison. Here, we show that the Li23 cell line possesses a distinct expression profile among hepatic cell lines.

METHODS

Cell culture

HUH-7, HUH-6, HEPG2, HLE, HLF and PLC/PRF/5 cells were cultured in Dulbecco's modified Eagle's medium supplemented with 10% fetal bovine serum. Li23 and PH5CH8 cells were maintained as described previously.[7] Cured cells (Li23-derived ORL8c and HuH-7-derived RSc), from which the HCV RNA had been eliminated by interferon (IFN) treatment, were also maintained as described previously.[7]

cDNA microarray analysis

Li23, ORL8c, HuH-7 and RSc cells (1×10^6 each) were plated onto 10-cm diameter dishes and cultured for 2 days. Total RNA from these cells were prepared using the RNeasy extraction kit (QIAGEN, Hilden, Germany). cDNA microarray analysis was performed according to the methods described previously.[7] Differentially expressed genes were selected by comparing the arrays from Li23 and HuH-7 cells. The selected genes were further compared with the array from ORL8c or RSc cells.

Reverse transcription polymerase chain reaction

Reverse transcription polymerase chain reaction (RT-PCR) was performed to detect cellular mRNA as described previously.[13] Briefly, total RNA (2 μg) was reverse-transcribed with M-MLV reverse transcriptase (Invitrogen, San Diego, CA, USA) using an oligo dT primer (Invitrogen) according to the manufacturer's protocol. One-tenth of the synthesized cDNA was used for PCR. The primers arranged for this study are listed in Table 1. In addition, we used primer sets for New York esophageal squamous cell carcinoma 1 (NY-ESO-1), β-defensin-1 (DEFB1), lectin, galactoside-binding, soluble 3 (LGALS3)/Galectin-3, melanoma-specific antigen family A6 (MAGEA6), UDP glycosyltransferase 2 family polypeptide B4 (UGT2B4), transmembrane 4 superfamily member 3 (TM4SF3), insulin-like growth factor binding protein 2 (IGFBP2), arylacetamide deacetylase (AADAC), albumin and glyceraldehyde-3-phosphate dehydrogenase (GAPDH), as described previously.[7]

RESULTS

Genes showing pronounced differences in gene expression between Li23- and HuH-7-derived cells

WE RECENTLY ESTABLISHED several Li23-derived cell lines showing robust HCV RNA replication.[7] In convenient microarray analysis using these cell lines, we noticed that the gene expression profile of Li23 cells differed considerably from that of HuH-7 cells, and that several genes, including cancer antigens such as NY-ESO-1 and MAGEA6, were highly expressed in Li23 cells but were not expressed in HuH-7 cells.[7] However, it

Table 1 Primers used for reverse transcription polymerase chain reaction analysis

Gene (accession no.)	Direction	Nucleotide sequence (5′–3′)	Products (bp)
Cancer antigen 45, A5	Forward	TGGAGATGACCTAGAATGCAG	218
(CT45A5); NM_001007551	Reverse	CTCGTCTCATACATCTTGCTG	
Four-and-a-half LIM domain 1	Forward	GGAATCACTTACCAGGATCAG	243
(FHL1; NM_001449)	Reverse	TTTGCAGTGGAAGCAGTAGTC	
Thymosin β4, X-linked	Forward	ACCAGACTTCGCTCGTACTC	179
(TMSB4X; NM_021109)	Reverse	TCGCCTGCTTGCTTCTCCTG	
Lectin, galactoside-binding, soluble 1	Forward	CAACACCATCGTGTGCAACAG	253
(LGALS1; NM_002305)	Reverse	CAGCTGCCATGTAGTTGATGG	
Interferon-induced transmembrane protein 2	Forward	CCTCTTCATGAACACCTGCTG	184
(IFITM2; NM_006435)	Reverse	CACTGGGATGATGATGAGCAG	
Apolipoproteins A1	Forward	ACTGTGTACGTGGATGTGCTC	273
(APOA1; X02162)	Reverse	CTTCTTCTGGAAGTCGTCCAG	
α-2-HS-glycoprotein	Forward	AACCGAACTGCGATGATCCAG	248
(AHSG; NM_001622)	Reverse	TTCGACAGCATGCTCCTTCAG	
Gap junction protein-α 1	Forward	CATCTTCATGCTGGTGGTGTC	253
(GJA1; NM_000165)	Reverse	GTTTCTGTCGCCAGTAACCAG	

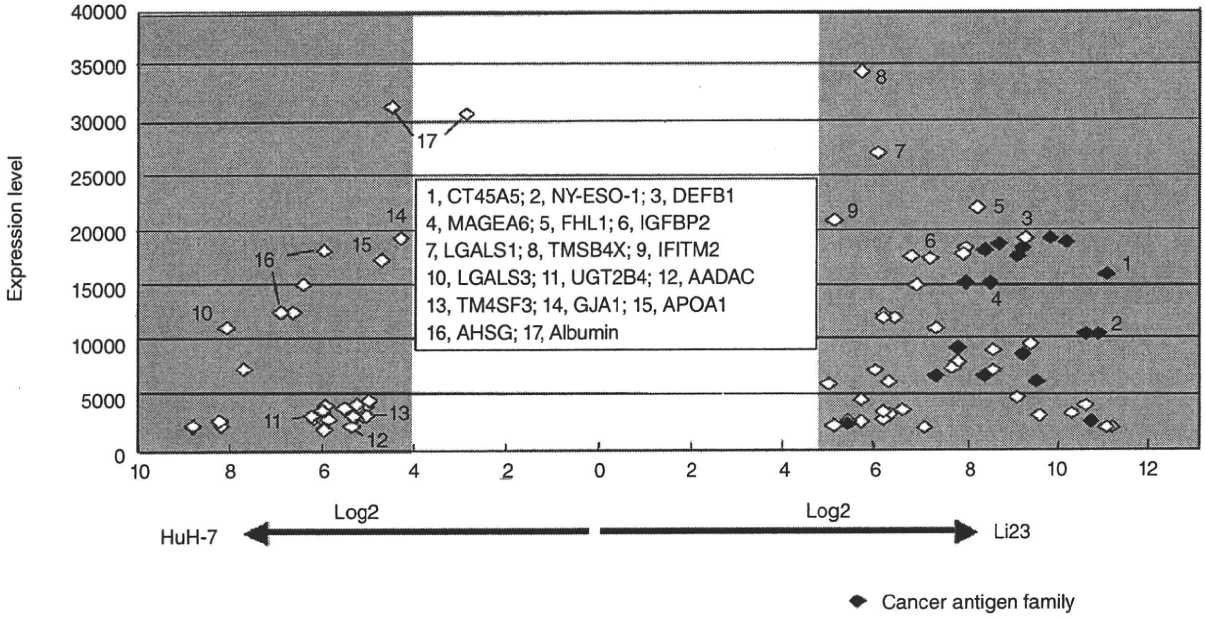

Figure 1 Genes showing pronounced differences in gene expression between Li23 and HuH-7 cells. The probes showing expression levels of more than 2000 and ratios of more than 30 (Li23/HuH-7) or 20 (HuH-7/Li23) are presented.

is unclear whether the expression profiles of these genes are characteristics of Li23 cells.

To clarify this point, comprehensive microarray analysis using Li23 and HuH-7 cells was performed. This revealed 4119 and 3570 probes whose expression levels were upregulated and downregulated at ratios of more than 2 and less than 0.5 in Li23 versus HuH-7 cells, respectively. From among these probes, we selected those showing ratios of more than 30 (Li23/HuH-7) and 20 (HuH-7/Li23), and further selected the probes showing expression levels of more than 2000 (actual value of measurement). By these selections, 80 probes were assigned (Fig. 1). The most distinguishing characteristic of the comparison is that the cancer antigen family (18 probes) was highly expressed in Li23 cells but was not highly expressed in HuH-7 cells (Fig. 1). From these probes, 14 known genes showing expression levels above 10 000 (#1–10 and #14–17 in Fig. 1) and three additional known genes (#11–13 in Fig. 1) were chosen as representative genes for further analysis.

Regarding the total of 17 genes, the expression levels in Li23 versus ORL8c or HuH-7 versus RSc were compared. The expression levels of most of the 17 genes were maintained between Li23 and ORL8c cells or between HuH-7 and RSc cells (Table 2). These results indicate that ORL8c and RSc cells retained the characteristics of parent Li23 and HuH-7 cells, respectively. However, it was notable that the expression levels of apolipoprotein A1 (APOA1), α-2-HS-glycoprotein (AHSG), and albumin were significantly higher in ORL8c cells than in Li23 cells, suggesting that ORL8c is selected as a specific clone from Li23 cell populations.

Expression profiles of representative genes whose expression levels showed drastic differences between Li23 and HuH-7 cells among human hepatic cell lines

Regarding the 17 genes selected above, we performed comparative analyses by RT–PCR using Li23, HuH-7, HuH-6, HepG2, HLE, HLF, PLC/PRF/5 and PH5CH8 cells in order to clarify whether or not these genes exhibit Li23-specific expression profiles. The results of the RT–PCR performed after optimization of PCR conditions in each gene resulted in the classification of the 17 genes into three types (A, B and C in Fig. 2). NY-ESO-1 and DEFB1 (high expression in Li23 only), and LGALS3/Galectin-3 (no expression in Li23 only) belonged to type A, which showed a Li23-specific feature. Type B showed that the expression levels in Li23, HLE, HLF, PLC/PRF/5 and/or PH5CH8 cells were greatly higher or lower than those in HuH-7, HuH-6 and HepG2 cells. Type B consisted of cancer antigen 45, A5

Table 2 Representative genes showing pronounced differences in gene expression between Li23 and HuH-7 cells

Gene	Accession no.	Li23	Li23-derived ORL8c	HuH-7	HuH-7-derived RSc
Cancer antigen 45, A5 (CT45A5)	NM_001007551	15 857†	10 508	8	23
Cancer testis antigen 1A (NY-ESO-1/CTAG1A)	U87459	9 005	5 503	5	8
β-Defensin-1 (DEFB1)	U73945	18 311	8 326	31	7
Melanoma-specific antigen family A6 (MAGEA6)	U10691	15 168	17 050	42	35
Four-and-a-half LIM domain 1 (FHL1)	NM_001449	21 851	13 428	77	79
Insulin-like growth factor binding protein 2 (IGFBP2)	NM_000597	17 429	8 931	117	13
Lectin, galactoside-binding, soluble 1 (LGALS1)	NM_002305	26 694	27 098	379	11
Thymosin β4, X-linked (TMSB4X)	NM_021109	34 273	26 199	648	307
IFN-induced transmembrane protein 2 (IFITM2)	NM_006435	20 762	9 645	595	637
Lectin, galactoside-binding, soluble 3 (LGALS3/Galectin 3)	BC001120	41	70	10 973	6 020
UDP glycosyltransferase 2 family polypeptide B4 (UGT2B4)	NM_021139	40	57	2 863	7 546
Arylacetamide deacetylase (AADAC)	NM_001086	57	73	2 282	4 746
Transmembrane 4 superfamily member 3 (TM4SF3)	NM_004616	95	51	3 220	1 265
Gap junction protein-α 43 KDa (GJA1)	NM_000165	951	2	19 090	19 485
Apolipoprotein A1 (APOA1)	X02162	673	7 230	16 920	15 202
α-2-HS-glycoprotein (AHSG)	NM_001622	308	6 373	18 436	26 000
Albumin	AF116645	4 304	30 111	30 234	33 140
	D16931	1 387	23 615	30 668	39 144

†Signal intensity in human genome U133 Plus 2.0 array.

(CT45A5), MAGEA6, four-and-a-half LIM domains 1 (FHL1), Thymosin B4, X-linked (TMSB4X), lectin, galactoside-binding, soluble 1 (LGALS1) and IFN-induced transmembrane protein 2 (IFITM2) – all of which were highly expressed in Li23 cells – and APOA1, AHSG and UGT2B4, which were highly expressed in HuH-7 cells. The remaining five genes were assigned to type C and showed more complex expression profiles (Fig. 2). For instance, Gap junction protein-α 43 kDa (GJA1) expression was observed in HuH-7, HLE, HLF, PLC/PRF/5 and PH5CH8 cell lines, but not in Li23, HuH-6 or HepG2 cell lines. In addition, IGFBP2 expression was observed in Li23, HuH-6 and PH5CH8 cell lines, but not in the other cell lines. Together, these results indicate that the Li23 cell line possesses a distinct expression profile among frequently used hepatic cell lines.

DISCUSSION

IN THIS STUDY, we assigned 17 known genes that showed drastic differences between Li23 and HuH-7 cells, and classified the expression profiles of these genes into at least three types among frequently used hepatic cell lines. Three genes (NY-ESO-1, DEFB1 and LGALS3/Galectin-3) were identified as the representative showing Li23-specific expression.

NY-ESO-1 is a well-characterized cancer-testis antigen (CTAG) that appears to be the most immunogenic CTAG known to date.[14] NY-ESO-1 is expressed in malignant tumors such as melanoma, lung carcinoma and bladder cancer, which are called "CTAG-rich" tumor types, but are expressed solely in the testis among normal adult tissues.[15] Because a spontaneous immune response to NY-ESO-1 is frequently observed in patients with malignant tumors including hepatocellular carcinoma,[16] cancer vaccine trials based on NY-ESO-1 are currently underway.[15] However, the biological role of NY-ESO-1 in both tumors and testis remains poorly understood. Accordingly, the Li23 cell line may be useful for the study of the biological role of NY-ESO-1.

Human defensins, which are small cationic peptides produced by neutrophils and epithelial cells, form two genetically distinct subfamilies, α-defensin and β-defensin. DEFB1, identified in this study, is one of six members belonging to β-defensins and appears to be involved in the antimicrobial defense of the epithelia of surfaces.[16,17] Although α-defensins consisting of six members are known to be expressed in a variety of tumors, DEFB1 is downregulated in some tumor types in which it could behave as a tumor suppressor protein.[18] Our study revealed that except DEFB1 in Li23 cells, no α- or β-defensin members were expressed in the

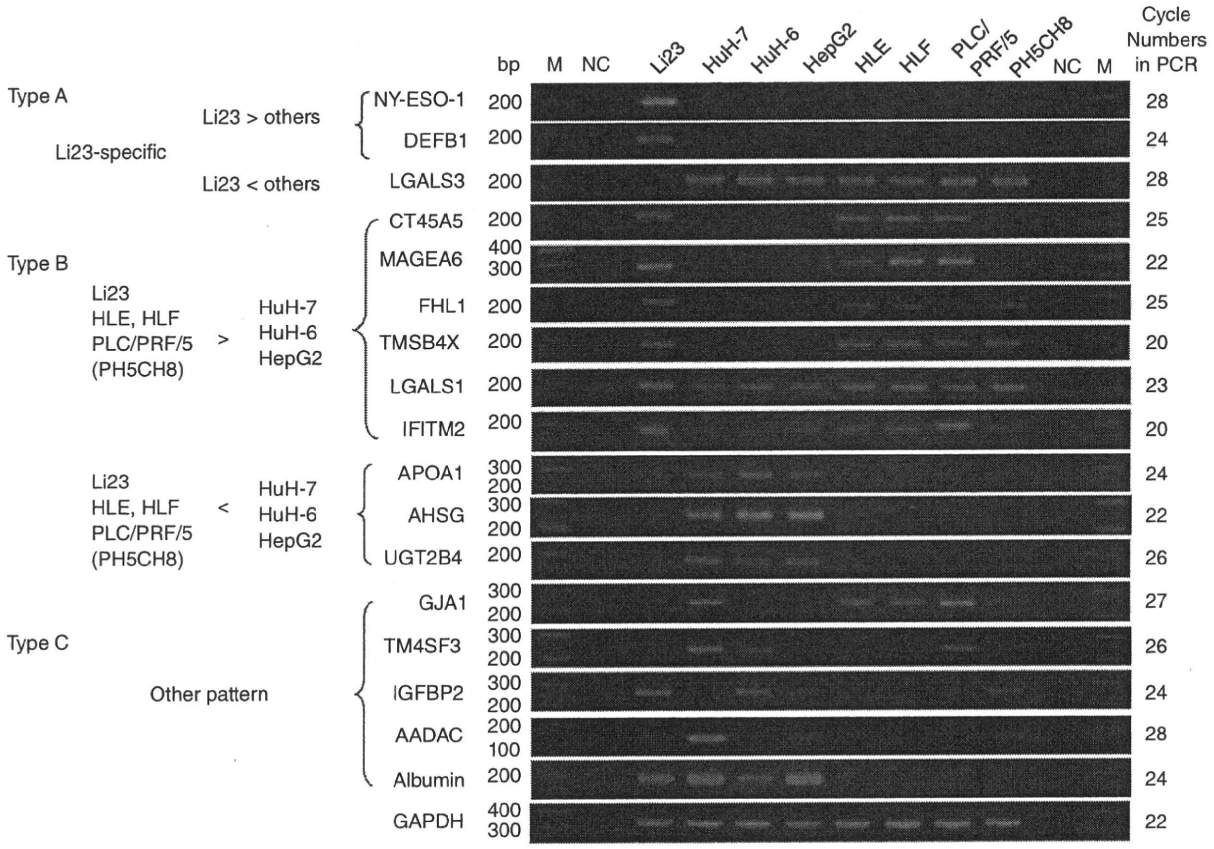

Figure 2 Expression profiles of representative genes, whose expression levels showed drastic differences between Li23 and HuH-7 cells, among human hepatic cell lines. Reverse transcription polymerase chain reaction (RT-PCR) analysis was performed as described in Methods. PCR products were detected by staining with ethidium bromide after separation by electrophoresis on 3% agarose gels.

hepatic cell lines tested in this study (data not shown). Because the molecular mechanism underlying DEFB1 expression or its role in oncogenesis remains to be clarified, Li23 cells may be useful for a study like that.

LGALS3/Galectin-3 is the most studied member of the galectin family, which is characterized by specific binding of β-galactosides through the carbohydrate-recognition domain.[19] LGALS3/Galectin-3 is ubiquitously expressed in numerous cell and tissue types; it is located in both nuclei and cytoplasm, and is secreted through a non-classical pathway. To date, LGALS3/Galectin-3 was found to be involved in many regulations including development, immune reaction, tumorigenesis, and tumor growth and metastasis.[19,20] Indeed, the overexpression of LGALS3/Galectin-3 in cirrhotic and hepatocellular carcinoma has also been reported.[21] In such situations, the absence of LGALS3/Galectin-3 expression in the Li23 cell line is a unique feature among hepatic cell lines, which show high expression levels. Accordingly, the Li23 cell line might be useful as a LGALS3/Galectin-3-null cell line for various studies including those on tumor growth and metastasis.

Although we identified Li23-specific genes showing distinct expression levels among hepatic cell lines examined, microarray analysis revealed that the expression profiles of Li23 and HuH-7 cells, both of which possess an environment for robust HCV replication, differed considerably. Accordingly, such differences may affect the properties or multiplications of HCV, such as susceptibility to anti-HCV reagents, the mutation rate of the HCV genome and the efficiency of HCV replication. Further comparative analysis using Li23 and HuH-7 cells will help to resolve these uncertain subjects.

ACKNOWLEDGMENTS

WE THANK NAOKO Kawahara for her technical assistance. This work was supported by a Grant-in-Aid for research on hepatitis from the Ministry of Health, Labor and Welfare of Japan. K. M. was supported by a Research Fellowship from the Japan Society for Promotion of Science for Young Scientists.

REFERENCES

1 Nakabayashi H, Taketa K, Miyano K, Yamane T, Sato J. Growth of human hepatoma cells lines with differentiated functions in chemically defined medium. *Cancer Res* 1982; **42**: 3858–63.
2 Lohmann V, Körner F, Koch J-O, Herian U, Theilman L, Bartenschlager R. Replication of subgenomic hepatitis C virus RNAs in a hepatoma cell line. *Science* 1999; **285**: 110–13.
3 Wakita T, Pietschmann T, Kato T *et al.* Production of infectious hepatitis C virus in tissue culture from a cloned viral genome. *Nat Med* 2005; **11**: 791–6.
4 Kato N, Sugiyama K, Namba K *et al.* Establishment of a hepatitis C virus subgenomic replicon derived from human hepatocytes infected in vitro. *Biochem Biophys Res Commun* 2003; **306**: 756–66.
5 Ikeda M, Abe K, Dansako H, Nakamura T, Naka K, Kato N. Efficient replication of a full-length hepatitis C virus genome, strain O, in cell culture, and development of a luciferase reporter system. *Biochem Biophys Res Commun* 2005; **329**: 1350–9.
6 Ariumi Y, Kuroki M, Abe K *et al.* DDX3 DEAD-box RNA helicase is required for hepatitis C virus RNA replication. *J Virol* 2007; **81**: 13922–6.
7 Kato N, Mori K, Abe K *et al.* Efficient replication systems for hepatitis C virus using a new human hepatoma cell line. *Virus Res* 2009; **146**: 41–50.
8 Tokiwa T, Doi I, Sato J. Preparation of single cell suspensions from hepatoma cells in culture. *Acta Med Okayama* 1975; **29**: 147–50.
9 Aden DP, Fogel A, Plotkin S, Damjanov I, Knowles BB. Controlled synthesis of HBsAg in a differentiated human liver carcinoma-derived cell line. *Nature* 1979; **282**: 615–16.
10 Doi I, Nambe M, Sato J. Establishment and some biological characteristics of human hepatoma cell lines. *Gann* 1975; **66**: 385–92.
11 Alexander JJ, Bey EM, Geddes EW, Lecatsaa G. Establishment of a continuously growing cell line from primary carcinoma of the liver. *S Afr Med J* 1976; **50**: 2124–8.
12 Ikeda M, Sugiyama K, Mizutani T *et al.* Human hepatocyte clonal cell lines that support persistent replication of hepatitis C virus. *Virus Res* 1998; **56**: 157–67.
13 Dansako H, Naganuma A, Nakamura T, Ikeda F, Nozaki A, Kato N. Differential activation of interferon-inducible genes by hepatitis C virus core protein mediated by the interferon stimulated response element. *Virus Res* 2003; **97**: 17–30.
14 Yoshida N, Abe H, Ohkuri T *et al.* Expression of the MAGE-A4 and NY-ESO-1 cancer-testis antigens and T cell infiltration in non-small cell lung carcinoma and their prognostic significance. *Int J Oncol* 2006; **28**: 1089–98.
15 Caballero OL, Chen YT. Cancer/testis (CT) antigens: potential targets for immunotherapy. *Cancer Sci* 2009; **100**: 2014–21.
16 Korangy F, Ormandy LA, Bleck JS *et al.* Spontaneous tumor-specific humoral and cellular immune responses to NY-ESO-1 in hepatocellular carcinoma. *Clin Cancer Res* 2004; **10**: 4332–41.
17 Bensch KW, Raida M, Magert HJ, Schulz-Knappe P, Forssmann WG. HBD-1: a novel bta-defensin from human plasma. *FEBS Lett* 1995; **368**: 331–5.
18 Droin N, Hendra JB, Ducoroy P, Solary E. Human defensins as cancer biomarkers and antitumour molecules. *J Proteomics* 2009; **72**: 918–27.
19 Dumic J, Dabelic S, Flögel M. Galectin-3: an open-ended story. *Biochim Biophys Acta* 2006; **1760**: 616–35.
20 Danguy A, Camby I, Kiss R. Galectins and cancer. *Biochim Biophys Acta* 2002; **1572**: 285–93.
21 Hsu DK, Dowling CA, Jeng KC, Chen JT, Yang RY, Liu FT. Galectin-3 expression is induced in cirrhotic liver and hepatocellular carcinoma. *Int J Cancer* 1999; **81**: 519–26.

Liver INTERNATIONAL
OFFICIAL JOURNAL OF THE INTERNATIONAL ASSOCIATION FOR THE STUDY OF THE LIVER

Liver International ISSN 1478-3223

BASIC STUDIES

Amino acid substitutions of hepatitis C virus core protein are not associated with intracellular antiviral response to interferon-α *in vitro*

Fusao Ikeda[1,2,3], Hiromichi Dansako[1], Go Nishimura[1], Kyoko Mori[1], Yoshinari Kawai[1,2], Yasuo Ariumi[1], Yasuhiro Miyake[2,3], Akinobu Takaki[2], Kazuhiro Nouso[2,3], Yoshiaki Iwasaki[2], Masanori Ikeda[1], Nobuyuki Kato[1] and Kazuhide Yamamoto[2,3]

1 Department of Tumor Virology, Okayama University Graduate School of Medicine, Dentistry, and Pharmaceutical Sciences, Okayama, Japan
2 Department of Gastroenterology and Hepatology, Okayama University Graduate School of Medicine, Dentistry, and Pharmaceutical Sciences, Okayama, Japan
3 Department of Molecular Hepatology, Okayama University Graduate School of Medicine, Dentistry and Pharmaceutical Sciences, Okayama, Japan

Keywords
antiviral activity – HCV core – hepatitis C virus – interferon

Correspondence
Fusao Ikeda, MD, Department of Gastroenterology and Hepatology, Okayama University Graduate School of Medicine, Dentistry, and Pharmaceutical Sciences, 2-5-1, Shikata-cho, Okayama 700-8558, Japan
Tel: +81 86 235 7219
Fax: +81 86 225 5991
e-mail: fikeda@md.okayama-u.ac.jp

Received 12 March 2010
Accepted 23 May 2010

DOI:10.1111/j.1478-3231.2010.02299.x

Abstract

Background: Studies on patients with hepatitis C virus (HCV) of genotype 1b have suggested that amino acids (aa) 70 and/or 91 of the HCV core protein affect the outcome of interferon (IFN)-α and ribavirin (RBV) therapy, although there are no clear supporting data *in vitro*. *Aims:* This study was designed to determine the differences among the antiviral activities of HCV core proteins with various substitutions at aa70 and/or aa91. *Methods:* The retroviral vectors expressing the HCV core proteins with substitutions of arginine/leucine, arginine/methionine, glutamine/leucine or glutamine/methionine at aa70/aa91 were transiently transfected or stably transducted into an immortalized hepatocyte line (PH5CH8), hepatoma cell lines and an HCV-RNA replicating cell line (sOR) to evaluate antiviral responses to IFN-α or IFN-α/RBV. Sequence analysis was performed using genome-length HCV-RNA replicating cells (OR6 and AH1) to evaluate HCV core mutations during IFN-α treatment. *Results:* The promoter activity levels of IFN-stimulated genes in the transiently transfected cells or the mRNA levels of 2′-5′-oligoadenylate synthetase in the stably transducted PH5CH8 cells were not associated with the HCV core aa70 and/or aa91 substitutions during IFN-α treatment. Antiviral responses to IFN-α or IFN-α/RBV treatment were enhanced in sOR cells stably transducted with the HCV core, although there were no differences in antiviral responses among the cells expressing different core types. Sequence analysis showed no aa mutations after IFN-α treatment. *Conclusions:* Antiviral activities were enhanced by HCV core transduction, but they were not associated with the HCV core aa70 and/or aa91 substitutions by *in vitro* analysis.

Hepatitis C virus (HCV) infection causes chronic hepatitis, and may progress to cirrhosis and hepatocellular carcinoma. More than 170 million people worldwide are infected with HCV, creating a serious global health problem (1, 2). Interferon (IFN)-α is widely used in the treatment of patients with chronic hepatitis C, and the current combination treatment with pegylated IFN-α and ribavirin (RBV) has improved the sustained virological response, and has a success rate of more than 50% (3). Despite this therapeutic success rate, however, there are still non-viral responders (NVR) to IFN-α treatment. High viral load and genotype 1 of HCV are major viral causes of IFN-α resistance. For patients with HCV genotype 1, variations in the amino acid (aa) sequence of the IFN sensitivity-determining region (ISDR) (4) and IFN/RBV resistance-determining region (IRRDR) (5) in the non-structural 5A region have also been reported as important predictors of therapeutic outcomes.

Recent studies on the virological features of HCV patients that are most predictive of NVR to IFN-α/RBV therapy (6, 7) proposed that HCV core protein aa70 and/or aa91 substitutions were independent and significant factors for therapeutic outcomes. In particular, substitutions of arginine by glutamine at aa70 and/or of leucine by methionine at aa91 were common in NVR. Patients with the HCV core aa70 substitutions often had a slow or no decrease in HCV-RNA levels during the early phase of IFN-α treatment (6–9). A previous report evaluating HCV dynamics during IFN-α therapy described a biphasic kinetic pattern of HCV-RNA decline, and the viral

decrease in the first phase was believed to be dependent on the direct effect of IFN-α on infected targets (10). We hypothesized that the types of HCV core proteins might alter the antiviral environment in the infected hepatocytes, and thus the aim of this study was to determine the difference in antiviral effects between HCV core proteins with various aa70 and aa91 substitutions.

Methods

Cell cultures

A non-neoplastic immortalized human hepatocyte line (PH5CH8) and hepatoma cell lines (HepG2, HuH-7 and Li23) were used to evaluate antiviral response, as described previously (11–13). We also used sOR cells harbouring subgenomic HCV-RNA derived from an HCV-O strain (genotype 1b) with Neo and *Renilla* luciferase genes (14). A schematic of the gene organization of sOR cells is shown in Figure 1a. All the cell lines used in this study were reported to possess the normal IFN signalling pathway (13–16). The cells were cultured in Dulbecco's modified Eagle's medium supplemented with 10% fetal bovine serum, penicillin, streptomycin and 0.3 mg/ml of G418 (Geneticin; Invitrogen, Carlsbad, CA, USA).

Plasmid constructions

Four retrovirus pCX4bsr vectors (17) expressing HCV core proteins were constructed, whose aa sequences were identical to the consensus sequences of the HCV core protein from the HCV-O strain encoding aa1–191, except for arginine at aa70/leucine at aa91 for CoreR70L91, glutamine at aa70/leucine at aa91 for CoreQ70L91, glutamine at aa70/methionine at aa91 for CoreQ70M91 and arginine at aa70/methionine at aa91 for CoreR70M91, as shown in Figure 1b. The two types of HCV core protein, CoreQ70L91 and CoreR70L91, were obtained from cells infected with serum HCV-O in a study of the dynamics of HCV populations during culture (18). CoreQ70M91 and CoreR70M91 were constructed from CoreQ70L91 and CoreR70L91, respectively, by PCR mutagenesis with primers containing base alterations. The sequences of these inserts were confirmed by Big Dye termination cycle sequencing using an ABI Prism 310 genetic analyzer (Applied Biosystems, Foster City, CA, USA).

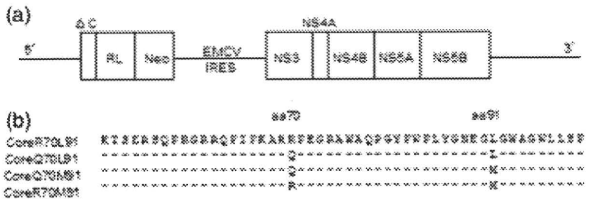

Fig. 1. Schema of subgenomic hepatitis C virus (HCV) RNA and partial aa sequences of the HCV core in the constructed retroviral vectors. (a) A schematic of the gene organization of subgenomic HCV replicon RNA. RL, *Renilla* luciferase; Neo, neomycin phosphotransferase; EMCV IRES, encephalomyocarditis virus internal ribosome entry site. (b) The partial aa sequences of the HCV core protein encoded in the constructed vectors. Four retrovirus pCX4bsr vectors expressing HCV core proteins were constructed, whose aa sequences were identical to the consensus sequences of the HCV core from HCV-O strain encoding aa1–191, except for arginine at aa70/leucine at aa91 for CoreR70L91, glutamine at aa70/leucine at aa91 for CoreQ70L91, glutamine at aa70/methionine at aa91 for CoreQ70M91 and arginine at aa70/methionine at aa91 for CoreR70M91.

Preparation of PH5CH8 cells and sOR cells stably expressing hepatitis C virus core proteins

PH5CH8 cells and sOR cells were infected with retrovirus vectors encoding different types of HCV core proteins, as described previously (19, 20). At 2 days post-infection, the culture medium was exchanged for a fresh medium containing blasticidin (20 μg/ml) for PH5CH8 cells or blasticidin (20 μg/ml) and G418 (0.3 mg/ml) for sOR cells. The culture was continued for 3 weeks so as to select the cells stably expressing the core proteins.

Quantitative reverse transcription-polymerase chain reaction analysis

Total cellular RNA was extracted using an Isogen extraction kit according to the manufacturer's protocol (Nippon Gene, Tokyo, Japan). The quantitative reverse transcription-polymerase chain reaction (RT-PCR) analysis was performed by real-time PCR using a Light Cycler (Roche Diagnostics, Mannheim, Germany) as described previously (20–22).

Luciferase reporter assay

For the dual luciferase assay, we used firefly luciferase reporter vectors encoding the 2′-5′-oligoadenylate synthetase (2′5′OAS) promoter, IFN-induced double-stranded RNA-activated protein kinase (PKR) promoter, IFN-stimulated response element (ISRE), and pRL-CMV, which expressed *Renilla* luciferase as described previously (15, 16). Plasmids were transiently transfected into the cells (2.0×10^4 cells/well in 24-well plates) using the FuGene6 transfection reagent (Roche Diagnostics) and cultured for 48 h. The cells were treated with human IFN-α (Sigma, St Louis, MO, USA) and/or RBV at the indicated doses for 6 h before harvest. The RBV was kindly provided by Yamasa (Chiba, Japan) (23). A whole cell lysate was prepared and assayed for firefly and *Renilla* luciferase activities according to the manufacturer's protocol (Promega, Madison, WI, USA). A Lumat LB9507 luminometer (Berthold, Bad Wildbad, Germany) was used to detect luciferase activity. The relative luciferase activity was normalized to the activity of *Renilla* luciferase. The data represent the means of the normalized luciferase activities of triplicate assays. The protocol for the *Renilla* luciferase assay to quantify HCV replicon

RNA was described previously (14). Briefly, 2.0×10^4 cells were plated onto 24-well plates in triplicate and were cultured for 12 h. The cells were treated with human IFN-α and/or RBV at the indicated doses for 48 h, and then harvested with *Renilla* lysis reagent (Promega) and subjected to a luciferase reporter assay according to the manufacturer's protocol. All the luciferase assays were repeated at least three times.

Western blot analysis

Preparations of cell lysates, sodium dodecyl sulphatepolyacrylamide gel electrophoresis (SDS-PAGE) and immunoblotting were performed as described previously (15, 16). The antibodies used in this study were those against Core (CP-11; Institute of Immunology, Tokyo, Japan), NS3 (Novocastra Laboratories, Newcastle, UK) and β-actin (AC-15; Sigma). Immuno-complexes were detected using the Renaissance enhanced chemiluminescence assay (PerkinElmer Life Science, Boston, MA, USA).

Cell proliferation analysis

The PH5CH8 cells (5.0×10^3 cells/well) or the sOR cells (2.5×10^3 cells/well) stably expressing HCV core proteins were plated onto 96-well plates, cultured for 24, 48 or 72 h and subjected to the colorimetric 3-(4,5-dimethylthiazol-2-yl)-2,5-diphenyltetrazolium bromide (MTT) assay according to the manufacturer's instructions (cell proliferation kit I; Roche) as described previously (24).

Results

No changes in the levels of interferon-stimulated genes were detected in response to the substitutions at hepatitis C virus core amino acid 70 and/or amino acid91 in transiently transfected cells

The constructed plasmids with the four different combinations of HCV core aa70 and aa91 substitutions were transiently transfected into PH5CH8, HepG2, HuH-7 and Li23 cells with lipofection. The levels of 2′5′OAS promoter activities were calculated as the luciferase activities at 48 h after transfection. As shown in Figure 2, the different types of HCV core proteins did not show clear differences in basal levels or enhanced levels with IFN-α stimulation, although the levels of CoreR70L91 transfection were slightly higher than the transfection levels for the other core proteins in PH5CH8 cells. As for PH5CH8 cells, we also evaluated the expression of HCV core proteins with Western blot analysis, and there were no obvious differences as shown in Figure 3. There were no differences either in the levels of the PKR promoter or in ISRE activities (data not shown). These results indicate that the levels of IFN-stimulated genes might not be affected by substitutions of the HCV core proteins at aa70 and/or aa91 in transiently transfected cells.

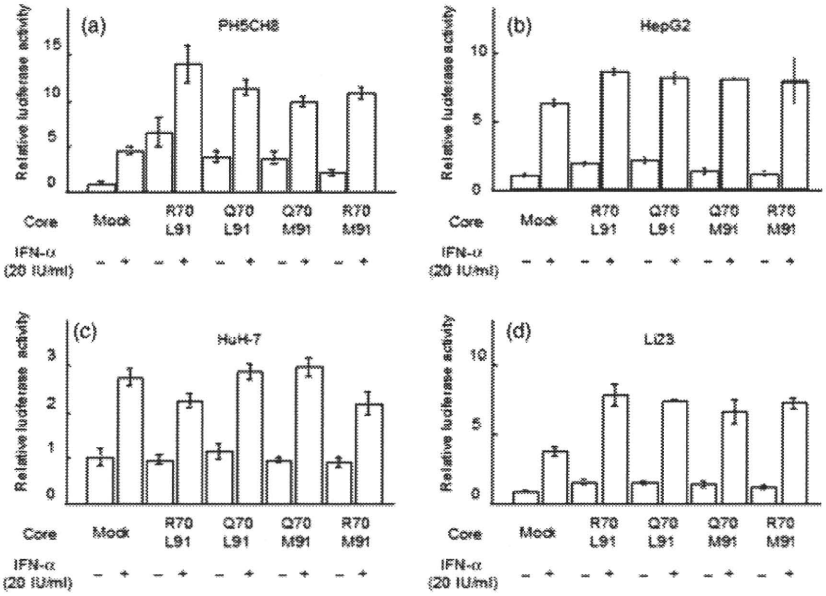

Fig. 2. 2′5′oligoadenylate synthetase (OAS) promoter activity of cells transiently transfected with the hepatitis C virus (HCV) core. The constructed plasmids with the four different types of HCV core aa70 and aa91 were transiently transfected into the cells (2.0×10^4 cells/well in 24-well plates) with lipofection. The cells were treated with IFN-α (20 IU/ml) for 6 h before harvest. The levels of 2′5′OAS promoter activities were calculated as the luciferase activities at 48 h after transfection. The figures show the results using PH5CH8 (a), HepG2 (b), HuH-7 (c) and Li23 cells (d).

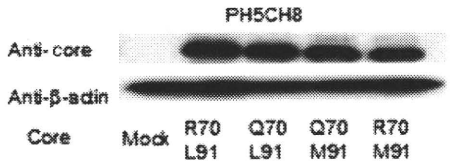

Fig. 3. The expression of hepatitis C virus (HCV) core proteins in the cells transiently transfected with the HCV core. The expressions of HCV core proteins were evaluated with Western blot analysis for PH5CH8. The constructed plasmids with the four different types of HCV core aa70 and aa91 were transiently transfected into the cells (2.0×10^5 cells/well in six-well plates) with lipofection. The cells were collected at 48 h after transfection.

The intracellular antiviral activities were augmented by hepatitis C virus core transduction, although they might not be affected by the amino acid 70 and/or amino acid 91 substitutions in the hepatitis C virus core stably transducted cells

To evaluate the interaction between the stable expression of HCV core proteins and intracellular antiviral activity, we prepared PH5CH8 cells that stably expressed HCV core proteins with retroviral transduction. The 2′5′OAS mRNA levels were measured with real-time LightCycler PCR and normalized with β-actin mRNA levels. As shown in Figure 4a, there were no clear differences in the basal levels or IFN-α-enhanced levels among the four transducted cell lines and the mock-transducted cells, although the expression levels of HCV core protein stably transducted cells were slightly higher than that of mock-induced cells. Western blot analysis showed that all these cell lines had similar levels of HCV core proteins (data not shown). Next, we monitored the association between the stable expression of HCV core proteins and RNA replication in an HCV replicon system. As we considered that a small difference of antiviral activity might be difficult to detect with real-time PCR, sOR cells were used for the monitoring. These cells are subgenomic HCV-RNA replicating cells with *Renilla* luciferase genes, and the replicon RNA can be quantified as luciferase activity. Measurement of luciferase activity is a useful and accurate means of quantifying the replicon RNA, because its sensitivity is much better than that of real-time PCR (14). We prepared the sOR cells expressing the HCV core proteins with retroviral transduction and stimulated the cells with IFN-α for 48 h. The level of antiviral activity, which was calculated as the median effective concentration (EC_{50}) of IFN-α, demonstrated that the cells transducted with the HCV core proteins showed a better response to IFN-α stimulation, but there was no difference in response among the cells expressing the different types of HCV core proteins, which is consistent with the results for the transient transfection of HCV core proteins (Fig. 4b). Western blot analysis demonstrated that the expressions of the HCV core and NS3 proteins did not show a clear difference among the sOR cells, irrespective of the types of HCV core proteins (Fig. 4c). As shown in Figure 4d, the results of the MTT assay demonstrated that the expressions of different types of HCV core proteins were not associated with cell proliferation in PH5CH8 cells or sOR cells. These results indicate that the intracellular antiviral activities are augmented in the presence of HCV core proteins, but they are not altered by the different substitutions at HCV core aa70 and/or aa91 in the cells stably expressing the HCV core.

Co-stimulation of interferon-α with ribavirin did not alter the association of hepatitis C virus core proteins with intracellular antiviral activity

Next, we hypothesized that co-stimulation of RBV might modulate the antiviral activity of the cells with different types of HCV core proteins. As shown in Figure 5, we evaluated the antiviral activity by quantifying HCV replicon RNA and 2′5′OAS promoter activity in the presence of IFN-α and RBV. The dose of RBV (20 μM) was determined based on the clinically used dose and the cell reactivity to RBV in our previous report (23). The HCV replications were suppressed (Fig. 5a), and the levels of 2′5′OAS promoter activities were enhanced (Fig. 5b and c) with a smaller dose of IFN-α, compared with IFN-α stimulation alone, indicating that RBV exerted an additive effect. Interestingly, the stimulation with RBV alone did not show any enhancement of 2′5′OAS promoter activity. These results indicate that the intracellular antiviral activities are augmented by costimulation with IFN-α with RBV, and that they are not altered by changes in the HCV core aa70 and/or aa91 substitutions.

Specific amino acid substitutions of hepatitis C virus core proteins were not detected in response to interferon-α treatment in the genome-length hepatitis C virus-RNA replicating cells

Next, we hypothesized that specific mutations in the HCV core region occur during IFN-α treatment. The two kinds of genome-length HCV-RNA replicating cells with different core aa70 and aa91 substitutions were cultured for 3 weeks with low-dose IFN-α stimulation, and then the core sequences were compared. We used OR6 and AH1 cells, both of which are genome-length HCV-RNA replicating cells (25, 26). OR6 cells have core proteins with glutamine at aa70 and leucine at aa91, corresponding to CoreQ70L91. AH1 cells have core proteins with arginine at aa70 and leucine at aa91, corresponding to CoreR70L91. After 3 weeks of culture with 12.5 IU/ml of IFN-α, several IFN-α- and G418-resistant colonies were obtained. We cultured them further without IFN-α stimulation and spread the colonies individually on 24-well plates. To examine the aa sequences of the core proteins in the colonies derived from OR6 and AH1 cells, RT-PCR was performed for the region encoding the HCV core protein, and the obtained PCR products were cloned into pBlueScript II, as described previously (27). The plasmid inserts of 10 clones each were sequenced. The results revealed that there were no specific changes of the aa sequence of HCV core